ALZHEIMER'S DISEASE:

AN EVALUATION OF MEMORY AND NEUROPATHOLOGY IN THE TgCRND8 TRANSGENIC MOUSE MODEL

by

Dr. Kathryn A. C. Glazner

A Thesis submitted to the Faculty of Graduate Studies

in partial fulfilment of the requirements of the degree of

MASTER OF SCIENCE

Department of Pharmacology & Therapeutics

Faculty of Medicine

University of Manitoba

ABSTRACT

Alzheimer's disease (AD) is a neurologically debilitating disease that is plaguing our elderly population. Transgenic mice with Alzheimer's disease mutations are used to study signal pathways, potential drug targets and mechanism of disease. However, studies of the effects of different AD mutations on behavior and neuropathological progression in mice have been inconsistent when comparing different genetic backgrounds. The aim of this study was to compare two commonly used TgCRND8 backgrounds, the 129SvEvtac/C57F1 and C3H/C57F1 strains, for memory function in the Morris water maze (MWM), and to determine differences in plaque burden. We found deficits in multiple parameters of the MWM in the 129SvEvtac/C57F1 strain. Similarly, this background strain showed significantly more amyloid beta (Aβ) plaque burden than the C3H/C57F1 strain. This supports the hypothesis that strain specific differences are apparent in spatial memory testing and neuropathologic progression of AD. It leads us to believe that epigenetics are key to understanding AD risk assessment and development.

ACKNOWLEDGEMENTS

I would like to start by thanking my supervisor Dr. Benedict C. Albensi for his mentorship and guidance throughout the course of my project. I thank you for the late night emails, working around my busy schedule and the autonomy to conduct my experiments.

To my committee members – Drs. Francis Amara and Don Smyth – I thank you both for your open door policy. For always being there when I had questions and needed to drop in on short notice. For your advice and support with both this degree and with my medical education. I am also grateful to Dr. Amara for the use of his lab, and the guidance of his graduate students in learning histochemistry.

A special note of thanks to Gary Odero for helping me with countless water maze trials that extended into weekends and the late nights performing imaging. I would also like to thank Dr. Jason Schapansky for teaching me molecular assays, and for being my "go-to-guy" for help trouble shouting and setting up the Albensi lab. I couldn't have done it without them.

I would like to acknowledge the Alzheimer's Society of Manitoba, the Scottish Rite Charitable Foundation and the St. Boniface Research Center Foundation for their financial support.

Lastly I thank my husband, Gordon, for his never-ending encouragement, positive outlook and support. Without him, this thesis would never have been completed.

Love you always.

To my family

TABLE OF CONTENTS

Page

LIST OF TABLES

LIST OF FIGURES

Page

LIST OF ABBREVIATIONS

Aβ……amyloid beta
ACI……...….annulus crossing index
AD……Alzheimer's disease
ADC……apparent diffusion coefficient
AICD……amyloid precursor protein intracellular cytoplasmic/C-terminal domain
Apoε……...…..Apolipoprotein Epsilon
APH1……anterior pharynx-defective-1
APP……..amyloid precursor protein
A2M.....alpha 2-macroglobulin
BACE……..beta-secretase
BIN……bridging integrator 1
CALM1..... calcium homeostasis modulator 1
cDNA.....copy DNA
CLAC-P……....collagen-like Alzheimer amyloid plaque component - precursor
CLU……..clusterin
CRND…….……Centre for Research in Neurodegenerative Diseases
CR1……complement component receptor 1 gene
C3H……....C3H/C57F1
DAPI ……..…4',6'-diamidino-2-phenylindole
DWI.....diffusion weighted imaging
EL.....escape latency
ER.....endoplasmic reticulum
FAD……..familial Alzheimer's disease
FOV.....field of view
IDE……insulin degrading enzyme
GAPDH…….…..glyceraldehyde-3-phosphate dehydrogenase
HSC……Health Science Center
LRP……lipoprotein receptor related protein
MAP……..microtubule associated protein
MMSE……...multi-slice single-echo
MRI……..magnetic resonance imaging
mRNA…….messenger RNA
MWM……..Morris water maze
NEP……neprilysin
NEX……..…….number of acquisitions
NFT……..neurofibrillary tangle
PBS……phosphate buffered solution
PCR……..polymerase chain reaction
PEN2……presenilin enhancer 2
PHF……...paired helical filaments
PICALM……phosphatidylinositol-binding clathrin assembly protein
PLG……plasminogen

PSEN1 or 2……..presenilin 1 or 2
qRT-PCR…..…….quantitative real-time polymerase chain reaction
ROI…….....region of interest
sAPPα or β……..……secreted APP alpha or beta
SBRC……..St. Boniface Research Center
SORL1…….…Sortilin-related receptor
SPSS……...…....Statistical Package for the Social Sciences
T……Tesla
TE……..….echo time
TR……..….repetition time
ThioS…….……Thioflavin S
129SvEv…….129SvEvtac/C57F1

LIST OF COPYRIGHTED MATERIAL (PERMISSION OBTAINED)

Figure 4 **-** Search strategies used by mice in the hidden platform portion of the Morris water maze. – Page 23**.** Figure reprinted from, Figure 1 on page 333 from Experimental Neurology: Morris water maze search strategy analysis in PDAPP mice before and after experimental traumatic brain injury by Brody & Holtzman, 2006 with permission from Elsevier Limited.

1. INTRODUCTION

1.1 Alzheimer's disease: Background and disease burden

Alzheimer's disease (AD) is a progressive and fatal brain disease in which patients suffer from loss of memory and decline in cognition. Frequently, confusion, disorganized thinking, impaired judgment, trouble communicating, and disorientation accompany cognitive loss to time, space and location. In addition, patients may exhibit marked changes in personality, such as paranoia or aggression, as well as both auditory and visual hallucinations. In the later stages of the disease, victims completely lose the ability to care for themselves, and eventually will lapse into coma and die, usually from respiratory complications. (Alzheimer's.Association 2008; Alzheimer's.Association 2009; Alzheimer.Society.of.Canada 2011). AD accounts for 60-80% of all dementias, and, it is estimated that 300,000 Canadians over the age of 65 have AD and that in 2008 alone, 97,000 Canadians developed AD or a related disease. These numbers are projected to grow with increasing frequency and it is projected that by 2031, this number will rise to over 750,000 Canadians (Alzheimer.Society.of.Canada 2011)

1.2 Pathology of Alzheimer's disease

Over one hundred years ago, Dr. Alois Alzheimer was the first to piece together the clinical aspects of behavioral and functional deterioration with post-mortem studies of his patient's brain including histopathological details. Dr. Alzheimer spent five years working with Auguste Deter who presented at age 51 with previously undescribed behavioral changes, including the loss of her short-term memory (Graeber 2003).

Alzheimer described it this way, “One of her first disease symptoms was a strong feeling of jealousy towards her husband. Very soon she showed rapidly increasing memory impairments. She was disoriented carrying objects to and fro in her flat and hid them. Sometimes she felt that someone wanted to kill her and would scream loudly. After four and a half years of sickness, she died” (Alzheimer 1907; Burns, Byrne et al. 2002). After her death, Dr. Alzheimer noted, “In the centre of an otherwise almost normal cell there stands out one or several fibrils due to their characteristic thickness and peculiar impregnability. Numerous small miliary foci are found in the superior layers. They are determined by the storage of a peculiar substance in the cerebral cortex” (Alzheimer 1906). These two features that Dr. Alzheimer first noted are known as neurofibrillary tangles (NFT) and amyloid beta (Aβ) plaques, which are still the pathological hallmarks of AD.

1.2.1 Neurofibrillary tangles

NFTs are made up of paired helical filaments (PHF) of microtubule associated protein (MAP) tau. In AD brain, tau exists in an abnormally hyperphosphorylated state secondary to decreased phosphatase activity or increased kinase activity, thus forming aggregates of insoluble polymers (Braak 1986; Grundke-Iqbal, Iqbal et al. 1986; Illenberger, Zheng-Fischhofer et al. 1998). These insoluble polymers aggregate with strain filaments to form intraneuronal, non-membrane bound neurofibrillary tangles. The MAP family of proteins are mainly found within neurons, and are believed to regulate neurite outgrowth and maintain neuronal morphology once mature (Tucker 1990). These tangles are found widespread throughout the AD brain, including in the entorrhinal

cortices, hippocampi, parahippocampal gyri, amygdalae, frontal, temporal, parietal and occipital associated cortices and certain subcortical nuclei projecting to these regions, all within the perinuclear cytoplasm as nonmembrane-bound bundles. It is believed NFTs first form predominately in the hippocampal formation, and subsequently in the anterior, inferior and mid-temporal cortex (Delacourte, Sergeant et al. 1998; Delacourte, David et al. 1999). NFTs occur in multiple non-AD pathology (ie. tauopathies) such as, Lewy body dementia, progressive supranuclear palsy, dementia pugilistica, frontotemporal dementia and Pick's disease, among others (Roberts 1988; Arai, Ikeda et al. 2001; Selkoe and Podlisny 2002; Williams and Lees 2009). Because of this, postmortem diagnosis of AD requires the presence of both NFTs and Aβ plaques, (Terry, Hansen et al. 1987; Markesbery 1997). It is likely that both Aβ and tau contribute to AD (Lee 2001). Research by Lewis et al. 2001 and Gotz et al. 2001 individually showed that Aβ deposits contributed to the formation of tau deposits in brain regions prone to AD pathology (Lee 2001). This is based on the observation that brains with AD plaques have excessive tau phosphorylation whereby tau loses its ability to properly bind microtubules within neurons, leaving the microtubules to deteriorate, and thus neuronal cell death quickly follows (Marx 2007).

1.2.2 Amyloid Beta plaques

Though hyperphosphorylated NFTs are associated with multiple dementias, senile plaques are widely believed to play a greater role in the pathology of AD (Hardy and Selkoe 2002). The primary component of senile plaques is the small peptide Aβ, a cleavage product from the larger transmembrane protein amyloid precursor protein

(APP). Amyloid plaques are associated with activated microglia, reactive astrocytes and dystrophic neuritis (Terry, Gonatas et al. 1964; Dickson 1997; Cummings and Cole 2002). Although plaques are a common brain feature in the elderly, those with AD exhibit markedly greater plaque numbers and density, to the extent that plaques are considered the hallmark differential diagnostic feature of AD.

1.2.2.1 Aβ formation

The formation and subsequent degradation of Aβ is a tightly controlled biochemical process, involving numerous enzymes in which Aβ metabolism appears to be the major function. APP is a transmembrane glycoprotein that has three major isoforms (695, 751 or 770 residues). It can be cleaved by α- or β-secretases, which are members of the disintegrin and metalloprotease family and cleave within the ectodomain. Cleavage of APP by α-secretase, produces secreted-APP-alpha (sAPPα), which demonstrates significant neurotrophic properties by promoting neurite outgrowth, synaptogenesis and cell adhesion (Mattson 1997; Gakhar-Koppole, Hundeshagen et al. 2008; Lichtenthaler 2011), and C83. The C83 component remains transmembrane until it is cleaved by the integral multimeric γ-secretase complex, composed of nicastrin, anterior pharynx – defective-1 (APH1), presenilin enhancer 2 (PEN2) and presenilin, an aspartyl protease and the catalytic subunit, to form P3 and amyloid precursor protein intracellular cytoplasmic/C-terminal domain (AICD) (Kaether, Haass et al. 2006). The Aβ form which is most fibrillogenic and displays the greatest neurotoxicity *in vitro*, and which is most associated with plaques in AD is the 42 amino acid $A\beta_{1-42}$. To generate $A\beta_{1-42}$ peptides, fibrils of these proteins must be proteolytically processed from the amyloid

precursor protein (APP) found on chromosome 21 (Maccioni, Muñoz et al. 2001; Hardy and Selkoe 2002) as shown in Figure 1.

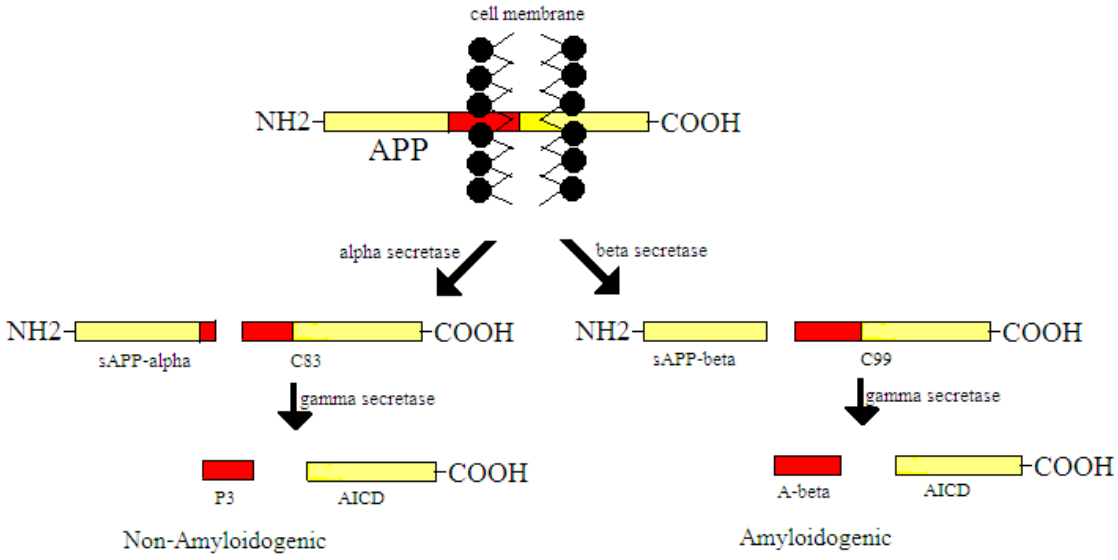

Figure 1 - Amyloid Precursor Protein Processing.
APP is a transmembrane protein that crosses the lipid bilayer between residues 700 and 723. It can either be cleaved by α-secretase to form sAPPα or β-secretase to form sAPPβ. The resultant transmembrane products are further cleaved by γ-secretase to produce P3 and AICD or Aβ and AICD, respectfully.

When APP is first cleaved by β-secretase (BACE), a membrane bound aspartyl protease; it is left susceptible to be sequentially cleaved by γ-secretase thus producing an amyloid-beta (Aβ) peptide. The BACE activity effectively produces the N-terminus of the C99 and the C-terminus of the secreted-APP-β (sAPPβ). The C99 N-terminus becomes the N-terminus of the Aβ peptide once cleaved by δ-secretase, but the length of the resulting Aβ peptide varies as δ-secretase has a "sloppy" cleavage site on the C-terminus end. Aβ peptides therefore have various lengths ranging from 36-43 amino acids long (Esch, Keim et al. 1990; Sisodia 1992; Selkoe 2001). Aβ40 is the most common isoform typically produced by cleavage in the endoplasmic reticulum (ER),

however it is the Aβ42 isoform which aggregates more quickly and is therefore more fibrillogenic. The Aβ42 isoform is typically cleaved in the trans-Golgi apparatus and contains two additional amino acids, isoleucine and alanine. It is more hydrophobic, the more amyloidogenic form of the peptide with more susceptibility to conformational change and most associated with disease states as components of neuritic plaques (Hartmann, Bieger et al. 1997).

1.2.2.2 Aβ clearance

There are three main enzymes known to have this function (Wang, Wang et al. 2010). Insulin-degrading enzyme (IDE), coded on chromosome 10, is a large zinc-binding protease M16A metalloprotease subfamily member that has recently been identified to degrade Aβ peptide (Farris, Mansourian et al. 2003). Mouse knockout studies of IDE have shown a 50% decrease in Aβ degradation and a corresponding cerebral accumulation of Aβ. Neprilysin (NEP), is another zinc-dependent metalloprotease enzyme that degrades Aβ, whose inhibition has also shown a greater deposition of Aβ42 in the brain (Iwata, Tsubuki et al. 2000). Three other enzymes implemented in this protective class include PLG protease, CLAC-P and Alpha-2M. The observation that there are numerous pathways in place for both formation and clearance of Aβ, and that this peptide is present as a normal part of human brain chemistry leads to the obvious conclusion that Aβ has a normal, but undiscovered, function. However, there are multiple lines of evidence, which indicate that Aβ can also cause neuropathology.

1.3. Early-onset familial Alzheimer's Disease

Another major piece of evidence that Aβ is critical to AD comes from inherited early-onset familial Alzheimer's disease (FAD). FAD accounts for less than 5% of AD presentations (Bertram and Tanzi 2008), and is caused by an inherited mutation with 100% penetrance. FAD is a much more aggressive form of the disease, presenting in younger (35-65 years) patients, progressing more quickly, and generally associated with greater incidence of complications, such as personality changes and hallucinations. It has the largest genetic basis, predominantly autosomal dominant, with three known causative mutations, all of which result in greatly enhanced production of $A\beta_{1-42}$.

1.3.1. APP

AD type 1 (10-15% of FAD) is caused by a missense mutations in the APP gene. Since these mutations occur on chromosome 21, individuals affected by Down's syndrome, who have three copies of chromosome 21, are more susceptible to AD (Kang, Lemaire et al. 1987). Similarly, non-Down's individuals with APP missense mutations typically present with symptoms starting from their late thirties to their late fifties (Selkoe 2001). These missense mutations occur near the Aβ region of the APP gene, and increase proportion of cleavage by γ-secretase, thus leading to an increase production of neurotoxic Aβ42 and increased formation of Aβ plaques (Chartier-Harlin, Crawford et al. 1991; Johnston, Cowburn et al. 1994; Wolfe and Guenette 2007).

1.3.2 Presenilins

Presenilin haloproteins, the proteolytically active component of γ-secretase as previously mentioned, are involved in the other two subtypes of FAD. The second

subtype, AD type 3 (30-70% of FAD) is caused by a mutation in the Presenilin 1 gene (PSEN1) located on chromosome 14q (Sherrington, Rogaev et al. 1995). The last subtype, AD type 4 (<5% of FAD) is caused by PSEN2 located on chromosome 1 (Levy-Lahad, Wasco et al. 1995; Rogaev, Sherrington et al. 1995; Van Broeckhoven 1995; Campion, Dumanchin et al. 1999; Larner and Doran 2006; Bird 2008). Together, the presenilin missense mutations alter γ-secretase cleavage, thus skewing production towards more Aβ42, and earlier pathological development (Wolfe and Guenette 2007). These individuals can also be affected in their thirties (Scheuner, Eckman et al. 1996; Selkoe 2001). The observation that all known FAD mutations result in increased $A\beta_{1-42}$ is persuasive evidence for the role of Aβ in AD, but perhaps the most compelling evidence comes from transgenic animals containing human FAD-linked genes.

1.3.3 Animal Models

Transgenic mice which contain human FAD-linked genes provide the most accessible animal model of AD (Duyckaerts, Potier et al. 2008). Though these animals do not completely or precisely replicate human AD pathology, they allow studies into Aβ-linked signaling pathways, underlying disease mechanisms, and potential drug targets.

The first class of transgenic mice used to study AD pathology was engineered to overexpress Aβ peptide via the insertion of FAD associated mutations. Those mice created to overexpress APP generally develop age-dependent amyloid deposition in the brain as well as thioflavin-S staining plaques, similar to those seen in human AD. Near these plaques, there are also dystrophic neuritis, reactive astrocytes and activated microglia (Reilly, Games et al. 2003). Two commonly used mice strains include the

PDAPP and Tg2576 lines which both show impairment in spatial memory behavioral testing, such as in water maze testing. Although these models develop similarities as described above, there are also differences. For example, the TgCRND8 mice (which express multiple APP mutations) develop parenchymal amyloid deposition at an earlier age, starting at 3 months (Chishti, Yang et al. 2001). There are also differences in proportion of Aβ40 versus Aβ42 production (Hsiao, Chapman et al. 1996). These differences between mouse lines are likely caused by different promoters, the effects of the different FAD mutations and the genetic backgrounds used to maintain the trangenes (Elder, Gama Sosa et al. 2010). Limitations of such mice as human AD models include the lack of tau neurofibrillary tangles, lack of neuronal death (at least at similar magnitude found in human AD) and there seems to be little affect on mouse life expectancy on certain background strains (Games, Buttini et al. 2006).

Transgenic models developed with a single presenilin mutation do not develop Aβ plaques. When crossed with plaque-forming APP lines, they cause earlier and more widespread plaque formation with a more neurotoxic Aβ42 than APP lines without PS1/2 mutations (Holcomb, Gordon et al. 1998). These bigenic mutants have earlier onset deficits in both water maze and Y-maze cognitive function (Arendash, King et al. 2001; Dineley, Xia et al. 2002).

The second class of transgenic mice used to study AD pathology, are transgenic mice engineered to express tau paired helical filaments, such as the JNPL3 line (Lewis, McGowan et al. 2000). These animals developed severe motor deficits likely due to axonal degeneration and loss of motor neurons in the spinal cord, but their tau conformation is not a true match to the NFTs seen in human AD. The creation of another

bigenic mouse strain combined Tg2576 (containing APP overproduction) with P310L (tau producers) producing the TAPP mice in order to investigate the effects of Aβ production on NFT pathology (Lewis, Dickson et al. 2001). In the TAPP mice, there are now NFTs in the hippocampus, subiculum and cortex – all regions burdened by Aβ plaque deposition and affected in the human AD brain.

Most recently, triple transgenic mice (3XTg-AD) combine the three mutations previously mentioned. They express the PS1 (M146V) mutation, the APP Swedish mutation and the tau (P301L) mutation (Oddo, Caccamo et al. 2003a; Oddo, Caccamo et al. 2003b). In the 3XTg-AD mice, amyloid beta plaques began to deposit by 6 months of age, before tau pathology that started at one year. Functionally, they developed age-dependent synaptic dysfunction with changes in long-term potentiation and impairments in spatial memory (Billings, Oddo et al. 2005). Even the closest transgenic mouse model to mimic human AD pathology is not the ideal model for disease. All transgenic mouse models are based on expression of mutant genes found only to be contributory to a small subset of human cases; those 5% of AD patients affected by FAD.

1.4 Late-onset AD

Though the discussion to this point has focused on FAD, by far the more prevalent form of this dementia is non-inherited, or late-onset AD, which accounts for 90-95% of cases. Late onset AD is believed to be sporadic but influenced by both environmental and genetic factors, which affect susceptibility to the disease, age of onset, and disease progression (Khachaturian, Corcoran et al. 2004; Carlo Lovati 2010). As the name implies, these cases tend to occur in later years (>65 years), and are not directly inherited,

at least not with 100% penetrance. Because this disease is primarily sporadic, and occurs late in life with a slow onset, it has been extremely difficult to identify risk factors for the disease. This multifactorial origin impedes development of either focused pharmaceutical agents that address the underlying pathology, or guidelines for lifestyle changes, which may protect against the disease. Nevertheless, through genetic analysis and epidemiology some progress has been made.

1.4.1. Genetic Risk Factors

Though only mutations in presenilin and APP cause strictly defined FAD (early onset, 100% penetrance) other genes have been identified which increase AD risk. The most well understood is the apolipoprotein E (Apoε) gene located on chromosome 19q, which has three alleles: ε2, ε3 and ε4. Apoε codes a protein involved in cholesterol metabolism. It also enhances the proteolytic breakdown of Aβ peptide, with the three isoforms displaying different efficiency. Apoε3/Apoε3 is considered neutral risk for AD. Whereas Apoε4 is the least effective proteolytically, thus allowing more accumulation of Aβ peptide, and a higher risk of developing AD. Those individuals who inherit two copies of Apoε4 are at a 20 times higher risk of developing the disease (Khachaturian, Corcoran et al. 2004; Lovati, Galimberti et al. 2010). Those with Apoε2 are protected against AD, but are at higher risks for certain cardiovascular conditions and abnormal lipid metabolism. Other potential genes under investigation include: SORL1, A2M and CALHM1 among others (Depboylu, Lohmuller et al. 2006; Rogaeva, Meng et al. 2007; Dreses-Werringloer, Lambert et al. 2008).

Sortilin-related receptor (SORL1), also known as LR11 and SORLA1, is a neuronal apolipoprotein receptor linked to the processing of APP, as it regulates its trafficking in endocytic compartments, thus affecting Aβ production (Andersen, Reiche et al. 2005; Offe, Dodson et al. 2006). It has been found that this receptor has significantly reduced expression in brain tissue of human AD patients (Scherzer, Offe et al. 2004). Specifically, this reduction was seen in sporadic AD, but not in cases of FAD, leading researchers to believe that SORL1 influences amyloid pathology independently from substrate-enzyme interactions found in FAD (Dodson, Gearing et al. 2006).

Alpha-2-Macroglobulin (A2M) is a panprotease inhibitor whose function is to degrade virtually any protease in the extracellular environment (Kovacs 2000). It also contains a specific Aβ binding site, which binds Aβ with high specificity. The activated Aβ-A2M complex can be internalized when binding to low-density lipoprotein receptor-related protein (LRP) (Narita, Holtzman et al. 1997), but A2M has also been shown to mediate Aβ independently from the LRP pathway (Qiu, Borth et al. 1996). Studies have also shown that LRP itself was associated with sporadic AD (Kang, Saitoh et al. 1997; Hollenbach, Ackermann et al. 1998). A2M contains two polymorphisms that increase the risk of developing sporadic AD by decreasing Aβ clearance (Kovacs 2000).

Calcium Homeostasis Modulator 1 (CALHM1) is coded on chromosome 10q24.33 and has been shown to encode a multipass transmembrane glycoprotein that controls cytosolic calcium ion concentrations as well as Aβ levels (Dreses-Werringloer, Lambert et al. 2008). It has been identified that the CALHM1 P86L polymorphism is associated with an increased susceptibility for developing sporadic AD, with an earlier age of onset, as it increases Aβ levels via an altered Ca^{2+} permeability (Boada, Antunez et al. 2010).

Within the last three years, four additional genes have been identified as contributing genetic predisposition for AD: Clusterin (CLU) on chromosome 8, complement component (3b/4b) receptor 1 gene (CR1) on chromosome 1, phosphatidylinositol-binding clathrin assembly protein (PICALM) and bridging integrator 1 (BIN1) (Lambert and Amouyel 2011).

1.4.2. Environmental and lifestyle risk factors

While a person can't modify their genetics, there are several other risk factors for sporadic AD in midlife that are determined by our environment and lifestyle, that may be modifiable (Bilbul and Schipper 2011). Metabolic risk factors include uncontrolled hypertension (systolic blood pressure >160 mmHg), cerebral ischemia/hypoxia, a sedentary lifestyle, lack of blood sugar control and hyperlipidemia. Studies have shown that individuals with uncontrolled hypertension have a significantly higher risk of AD in later years (Kivipelto, Helkala et al. 2001) and epidemiological studies have revealed that antihypertensive medications in patients with cardiovascular disease may be dementia protective (Tzourio, Anderson et al. 2003; Whitmer, Sidney et al. 2005). Individuals who have suffered stroke or transient ischemic attacks are also at an increased risk of developing AD, likely due to cerebral hypoxia, which is theorized to increase the expression of BACE1 and thus Aβ production (Kalaria 2000; Sun, He et al. 2006). Physical activity is neuroprotective against one's risk of AD through reducing vascular co morbidities (Kivipelto, Helkala et al. 2001) as well as enhancing neurotrophic factor gene expression, promoting neuroplasticity, decreasing Aβ burden (Rovio, Kareholt et al. 2005). However, it should be mentioned that the level and amount of exercise needed to

be beneficial is controversial. Diabetes is also another known risk factor where those Apoε4 positive individuals are at two-fold increased risk of developing AD, than those without type-2 diabetes (Peila, Rodriguez et al. 2002). Lastly, high cholesterol is also a risk factor independently of APOE status (Kivipelto, Helkala et al. 2002). It seems as a general rule, that what is good for your heart is also good for your brain.

Nutrition may also play a role. It has been suggested that low blood levels of folic acid and increased levels of homocysteine may be risk factors for sporadic AD (Clarke, Smith et al. 1998; Wang, Wahlin et al. 2001). The later can be successfully lowered with oral supplementation with folic acid, and vitamins B12 and 6 (Tucker, Olson et al. 2004). However, it is also believed that these three supplements are only beneficial for those deplete in these nutrients (Ford, Flicker et al. 2010). Antioxidants are well known by the general population to be beneficial to preventing AD. Studies have found that both a moderate consumption of coffee (three to five cups per day) and red wine (250 – 500 ml/day) are potentially advantageous to ward off AD (Maia and de Mendonca 2002; Larrieu, Letenneur et al. 2004; Eskelinen, Ngandu et al. 2009).

Other beneficial tasks that can contribute to stalling the age of onset of AD are those that 'work out' our brain. Robust mental activity, such as years of formal education, cognitive engagement and social stimulation all contribute to increase cognitive reserve (Bilbul and Schipper 2011). Formal education, such as at the post-secondary level, aides to increase cognitive reserve directly by influencing neural growth and synaptic plasticity (Crowe, Andel et al. 2003). Cognitive exercises or 'brain-training exercises' (such as reading, playing musical instruments and doing crosswords) showed a 50% reduction for dementia (Valenzuela and Sachdev 2006) and are quite easy to perform on a regular

basis. Social interaction is also neuroprotective, including such activities as playing board games or taking part in group discussions (Wilson, Krueger et al. 2007).

Many of the above mentioned lifestyle choices are beneficial not only to prevent AD, but also for our overall health. Many of these risk factors stress the importance of epigenetic in disease development. The importance is to realize that for 95% of the population (those of us at risk for sporadic late onset AD), we can still modify our risks by making healthy lifestyle changes. And much research is still needed to determine how these risk factors are affected by our unique genome.

2. STATEMENT OF HYPOTHESIS

In this study we used the TgCRND8 mouse model of AD, and it is readily available at our institution. This mouse model originated at the University of Toronto (see Methods and Materials), but has been bred for numerous generations in our animal facility. The TgCRND8 model is a popular AD mouse model; it contains two amyloid precursor protein (APP) mutations ('Swedish' KM670/671NL + V717F 'Indiana') resulting in robust amyloid beta plaque deposition starting at 3 months of age. These mutations have been inserted into a variety of mouse background strains resulting in different phenotypes in behavioral testing (Chishti, Yang et al. 2001)

We investigated two TgCRND8 mice on different background strains (C3H/C57F1 and 129SvEvtac/C57). These strains were compared with regards to behavioral testing of spatial memory formation, plaque burden and APP/IDE expression. We hypothesized that both the background strain and sex of the TgCRND8 mouse model of Alzheimer's disease would impact behavioral performance in the Morris water maze due to different levels of mutational expression. We did not, however, postulate, which would perform worse, which would have more plaque burden, or which, would have higher/lower level of APP/IDE expression.

We lastly performed a separate pilot MRI study to investigate in these TgCRND8 mice as to whether our MRI system was powerful enough to visualize plaque deposition and corresponding apparent diffusion coefficient difference. We did expect to visualize plaques, and we expected to have an increased ADC value in the transgenic mice.

3. METHODS AND MATERIALS

3.1 Animal Breeding and Housing

All animal studies were performed under a protocol approved by the University of Manitoba Protocol Management and Review Committee. All mouse lines originated from Dr. David Westaway at the Centre for Research in Neurodegenerative Diseases (CRND, University of Toronto) as previously described (Chishti, Yang et al. 2001). All mice were engineered to express a double mutant form of amyloid precursor protein 695 ("Swedish" KM670/671NL+V717F "Indiana") directed by the hamster PrP gene promoter (Chishti, Yang et al. 2001). The APP_{695} cDNA cassette was inserted into the oocytes of different genetic backgrounds resulting in our possession of TgCRND8 mice on two different backgrounds; 129SvEvtac/C57F1 and C3H/C57F1 for their use in these studies. See Table 3 in Appendix for a complete list of mice used and their specific genotypes. While mice were housed at SBRC, they were fed standard mouse pellets *ad libitum* and communally caged in groups of 2-4 mice unless separation was required due to fighting behavior as seen by some male mice. All cages were supplied with either a plastic cylinder or cardboard house insert to provide shelter and enrichment.

3.1.1 Animals Used for Behavior Studies.

It should be noted that the mice used in our behavioral experiments were bred at two different locations, CRND and SBRC. Those bred at the CRND were shipped to our HSC facility in adulthood, and aged to one year of age. Those bred at SBRC were aged to three months or one year, and then transferred to HSC for behavioral experimentation

3.1.2 Animals Used for Magnetic Imaging.

All animals used for MRI studies were bred at SBRC. Young, pre-plaque (3 months old) versus older control and TgCRND8 animals (12-16 months) all on C3H/C57F1 background were used for these studies. Thirteen older mice were imaged with diffusion-weighted MRI of which 11 datasets were usable (4 female wild-type and 7 male TgCRND8). Twelve mice (six 13-months old and six 3-month old) were imaged with high-resolution T2-weighted imaging (3 wild-type and 3 transgenic in each group).

3.2 Morris water maze

The MWM for behavioral testing of hippocampal dependent spatial memory was first developed and described by R. Morris in 1984 (Morris 1984). The idea behind the test is that when a mouse is placed in a pool of water, it will try to escape since the water acts as an aversive stimulus. A hidden platform placed slightly below the surface of the water (made opaque with food coloring, etc.) serves as a potential means of escape, and once they find and mount the hidden platform, they are able to climb out of the water. The testing occurs in 2 phases. At first, mice randomly swim in the MWM and eventually find the hidden platform by chance (acquisition phase). However, as a result of repeated exposure to the MWM, the mice are able to find the location of the platform more quickly using spatial cues from their surroundings. Once they start to develop a so-called mental spatial map of their surroundings, their accuracy and speed of remembering the location of the hidden platform increases as seen by a decrease in the overall path length and amount of time it takes the mice to find the target (i.e. escape latency). Then, the

platform is removed and the animals are tested again to see if they recall the location of the missing platform (retention phase).

3.2.1 Design

Our MWM testing was conducted in an 83 cm (diameter) circular white polyethylene tank, purchased and modified by Polywest Canada, Winnipeg, Manitoba. Other groups have used tanks ranging from 61-150 cm for studies involving mice (Means, Higgins et al. 1993; D'Hooge, Franck et al. 1999). The tank was 65 cm in height, and for the purpose of our experiment, it was filled with water (24-25˚C) to a depth of 30 cm. The water was made opaque with powdered skim milk powder, made fresh daily. Our visual cues consisted of four distinct colored shapes: a yellow arrow, a green triangle, a blue circle and a red star. The cues were positioned equidistance apart, 25 cm above water level within the polyethylene tub. Other external visual cues were extinguished with a black curtain hung from the ceiling above, which hung to 10 cm below the top rim of the pool (see Figure 2). The room housing the maze was lit with three fluorescent bulbs positioned outside of the curtain, providing diffuse light above and through the plastic wall of the tank. A WebCam was positioned above the water surface in the center of the tank, zoomed to capture the entire water surface area of the maze. Video footage was recorded during the experiment and then analyzed subsequently on a laptop computer.

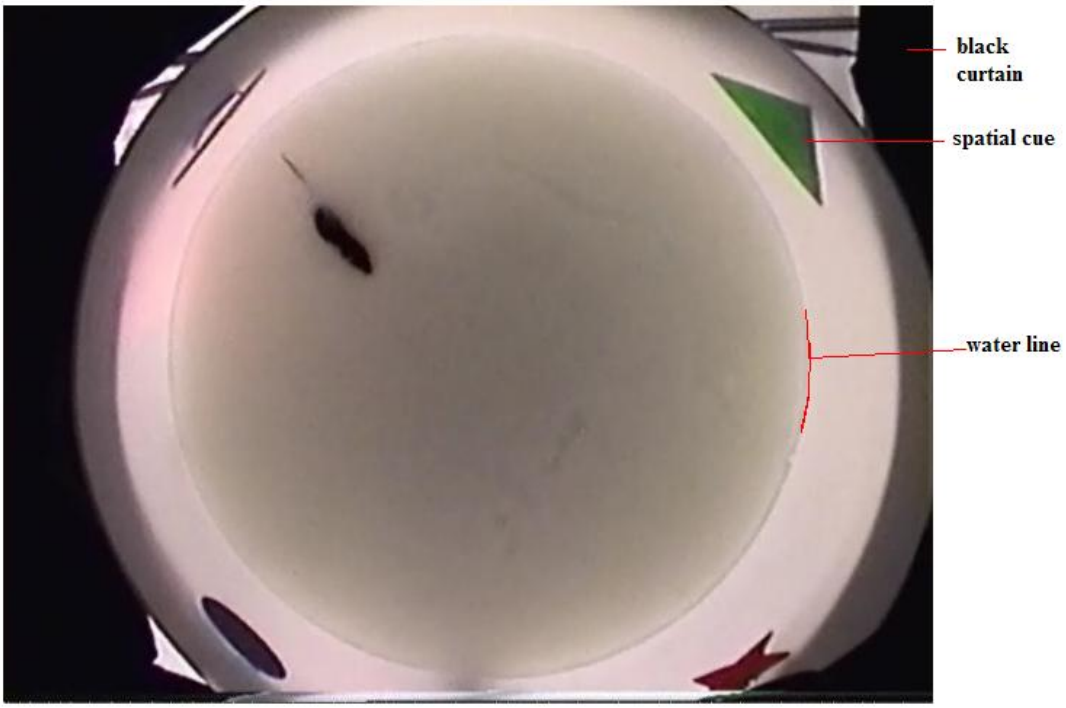

Figure 2 Design of the Morris water maze.
A circular pool filled with white opaque water. There are four external visual cues, and a black curtain extinguishing uncontrolled external stimuli.

3.2.2 Acquisition Phase

The acquisition phase of the MWM is conducted over seven days. During this time, a hidden Plexiglas platform (covered with cheesecloth for additional grip) measuring 5 cm in diameter is submerged, 1 cm below water level. This platform remained fixed in location throughout all the experiments (Figure 3**)**.

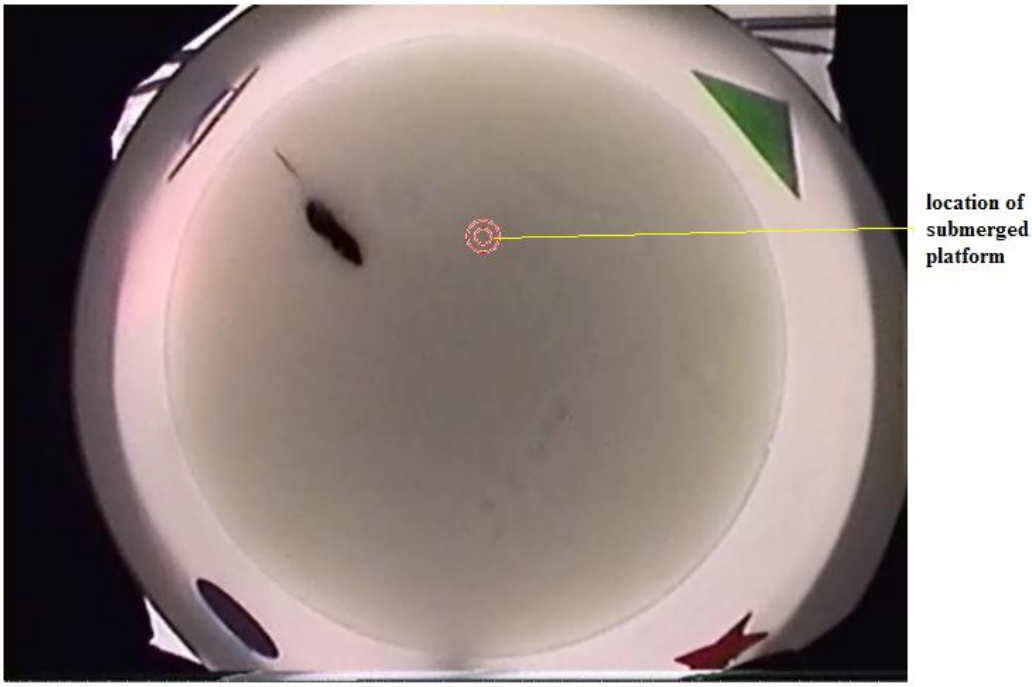

Figure 3 Location of Submerged Platform during Acquisition Phase

During each trial a mouse was introduced to the maze for 90 seconds. Four trials were conducted each day. The time between trials was 30 minutes, and all trials were performed in the morning hours between 9 am and 12 pm. The mice were placed into the water tail first to decrease stress and randomly placed at one of the four designated start locations (i.e., in front of the four respective visual cues), once daily. They were allowed 90 s to find the platform, after which time, they were aided to the platform by the hand of the experimenter. In either situation, the mouse had to sit on the platform for 10 s before it was returned to its cage where it was placed under a heat lamp to dry off. The mice were also allowed to self-groom to remove the milk that had adhered to their coat. During the acquisition phase, there were two parameters that were measured. The first was the escape latency (EL), which was the amount of time in seconds that it took the mouse to

find the hidden platform. For those mice that did not find the hidden platform, a score of 90 s was given. Another parameter encoded and measured was the Search Strategy, which was an analysis of the path taken by the mouse to find the missing platform. Brody & Holtzman described three different categories of search strategies as spatial strategy, non-spatial, systemic strategy and strategies based on repetitive looping, see Figure 4 (Brody and Holtzman 2006).

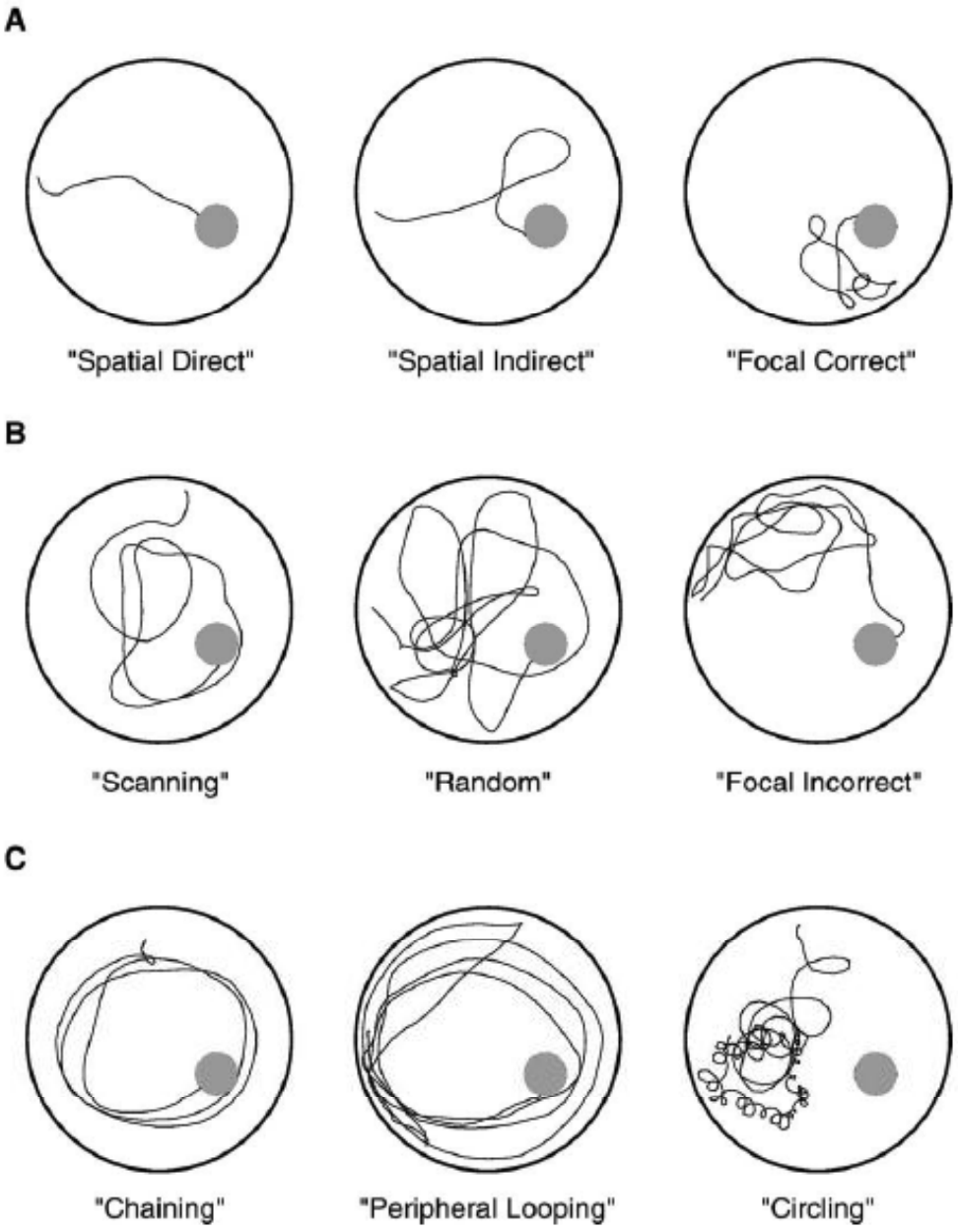

Figure 4 Search strategies used by mice in the hidden platform portion of the Morris water maze

The filled gray circle shows the location of the platform. (A) Spatial strategies. (B) Non-spatial, systemic strategies. (C) Strategies based on repetitive looping. Figure reprinted from, Experimental Neurology, Brody & Holtzman, Morris water maze search strategy analysis in PDAPP mice before and after experimental traumatic brain injury, Figure 1, pg 333, copyright (2006) with permission from Elsevier Limited.

One experimenter (Gary Odero- technician- Albensi lab.) blinded to genotype and background strain assigned a predominant search strategy to each trial of the acquisition phase for all mice in this study as described previously (Wolfer and Lipp 2000; Graziano, Petrosini et al. 2003; Janus 2004; Brody and Holtzman 2006). To further describe these categories as per Brody & Holtzman, spatial strategies (Figure 4A) were those where the mouse either swam directly to the platform ('spatial direct'), swam to the platform with at most a single loop ('spatial indirect') or they swam directly to the correct target quadrant as per Figure 5, and searched that quadrant for the platform ('focal: correct target quadrant'). Systemic but non-spatial strategies (Figure 4B) were those where the mouse searched interior portion of water surface area without spatial focus ('scanning'), searched the entire tank without spatial focus ('random') or searched a small incorrect area of the tank that did not house the hidden platform ('focal: incorrect target quadrant'). The last category, were those based on repetitive looping, and included mice who swam a circular route at an approximately fixed distance greater than 15 cm from the wall ('chaining'), those that swam circular routes within that 15 cm from the wall ('peripheral looping') and those who swam tight circles/ corkscrew-like patterns, which might have had some overall direction to their movement ('circling').

Any mice found to displace a "true thigmotaxis" whereby they hugged the wall of the tank – guided by touch, were categorized as peripheral looping, similar to the categorization scheme of Brody & Holtzman. For analysis of data collected in the acquisition phase, EL was graphed using Excel, Microsoft Office 2003, where an average EL value was calculated per day (block) of experiment (each block was composed of 4

trials). Statistical analysis was performed using SPSS13, where 2-Way ANOVA with repeated measures was applied.

3.2.3 Retention Phase

The retention phase of the MWM was conducted over three days, which was immediately started after the acquisition phase ended. During this phase, the hidden platform was removed from the water in order to test the animal's ability to recall the location of the platform. To this end, the mice were reintroduced to the pool for 4 trials of 90 seconds, 30 minutes apart. Over this 90 s period, the mouse was left to search for the missing platform. Once the 90 seconds expired, the mouse was removed from the pool, and returned to its cage.

There are three parameters that were measured from the video recordings of the retention phase. The first parameter was the number of times the mouse passed over the location of the missing platform, as gauged by a superimposed pattern as outlined by two concentric circles, as seen in Figure 5.

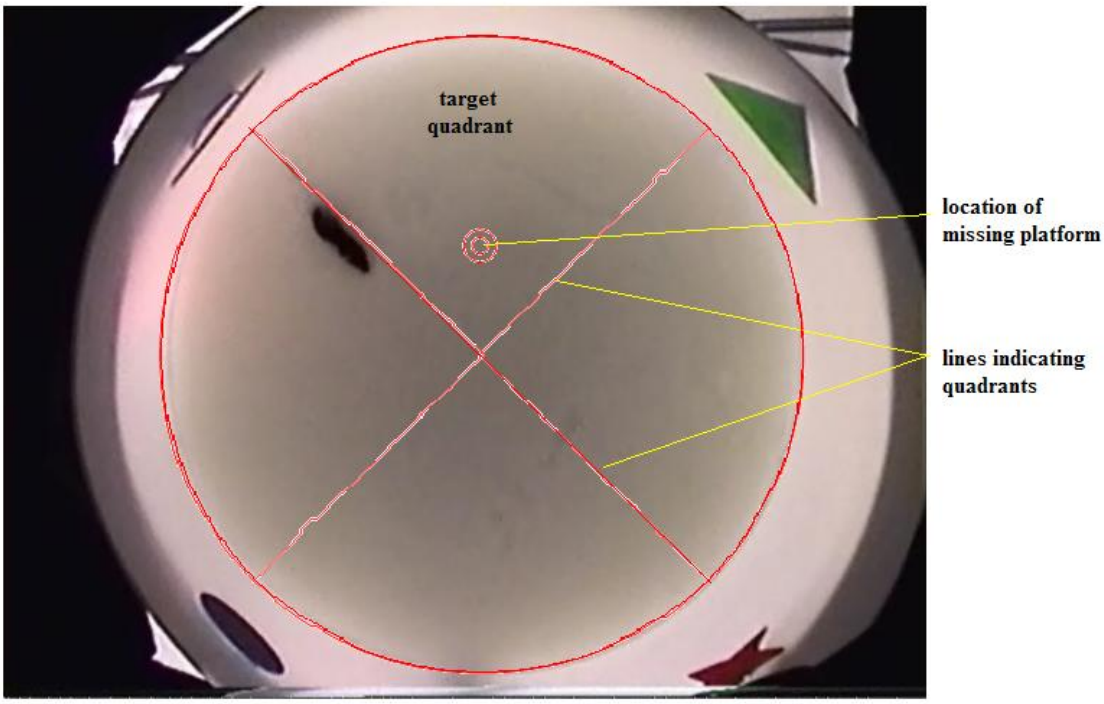

Figure 5 Location of missing platform and outline of quadrants superimposed in the retention phase of the Morris water maze.

For the pass over the platform to count as an official scoring pass, the mouse's body must fully cover the inner circle. The second parameter measured was the amount of time the mouse spent in the target quadrant, as depicted in Figure 5. This parameter was measured using a stopwatch and was defined by the mouse passing half of its body area into the target quadrant. The last parameter measured was the Annulus Crossing Index (ACI). The ACI is a calculated ratio of the number of times the mouse crosses the missing platform site in the target quadrant minus the mean of passes over alternative platform sites in non-target quadrants (Wehner, Sleight et al. 1990; Gass, Wolfer et al. 1998; Chishti, Yang et al. 2001). A positive ACI value indicates a selective focal search of the previous platform position, while an index approximating zero indicates nonspatial or circular searching of the maze.

3.3 Histology

3.3.1 Slice Preparation

Mice used for histological staining were anaesthetized with vaporized isofluorane and then perfused using standard techniques. Isofluorane was first administered with a nose cone and the animal was determined anesthetized when a loss of toe pinch reflex was confirmed. Next, the mice were pinned down and a thoracic incision made to expose the heart. The right atrium was nicked and 30 ml of formalin was pumped via syringe into the left ventricle until the fluid draining from the atrium was clear. The animal was then decapitated and the brain excised. The forebrain and cerebellum were dissected out and the remaining third of the brain was paraffin embedded and later sliced coronally to 6-8 μm with a microtome to include a cross section of the hippocampus. The sections were mounted on SuperFrost slides (Fisher Scientific) and stored at room temperature. For the year old TgCRND8 mice in the background strain study, one mouse from each group was used, for a total of four 129SvEvtac/C57F1 mice and four C3H/C57F1 mice; half were controls and half were transgenic for each background strain, after completion of the MWM. For those imaged from the MRI study, two representative samples were prepared from each the transgenic and littermate groups.

3.3.2 Staining

Prior to staining, all sample slides were dewaxed with xylene three times for 5 minutes each and rehydrated with successive 5 minute washes of decreasing ethanol solutions (100%, 95%, 70%, 50% and 30%). The slides were rinsed twice with phosphate buffered solution (PBS tablets – MP Biomedicals Inc., Solon, Ohio, USA). Auto

florescence was removed with a 5 minute wash of 0.5% $NaBH_4$ (Acros Organics, New Jersey, USA) followed by two rinses with PBS. All slides were stained with two dyes. The nuclei were first stained blue with 1µg/ml of 4,6-diamidino-2-phenylindole (DAPI - Calbiochem, EMD Biosciences, Inc. , La Jolla, CA, USA) for 10 minutes. Staining with DAPI was to enable identification of the granule cell layer in the hippocampus for image processing. For the behavioral mouse samples, the slides were washed twice with PBS and the amyloid beta plaques were stained "apple green" with filtered 0.01g/ml of Thioflavin S (Sigma, St. Louis, MO, USA) for 5 minutes (Wall 1996). Samples from mice scanned with MRI, were also washed with PBS, but amyloid beta plaques were stained with Congo Red. All slides were differentiated with 70% ethanol, rinsed twice with ddH_2O, and mounted with cover slips using Prolong Gold antifade reagent (Invitrogen Molecular Probes, Eugene, Oregon, USA).

3.3.3 Imaging

All images were captured within 24 hrs of staining. For the mice scanned with MRI slides, five slides per brain were imaged utilizing a fluorescence microscope using a DAPI filter at 323 nms (ie. to visualize cell nuclei thus identifying the hippocampus region) and a Texas Red filter at 520 nms to visualize the plaques stained with Congo Red. The resulting images were overlaid in order to visualize cell structure and plaque deposition/character together in one image.

For the behavioral mouse slides, minimums of five slides per brain for each group (ie. controls and transgenics for each background strain, 129SvEvtac/C57F1 and C3H/C57F1) were imaged. A fluorescence microscope using a DAPI filter at 323 nms

was used for imaging at the hippocampal region. Plaque quantification was determined using custom MatLab software (coded by Everet Anema – student of Dr. Derek R. Oliver).

3.4 Magnetic Resonance Imaging

3.4.1 Apparatus

Imaging was performed using a 7 Tesla horizontal Bruker magnet and Biospec/3 console (Biospin GmbH, Ettlingen, Germany) running Paravision 2.0.1 acquisition software. The MR probe used was a custom built quadrature volume coil (length 3.0 cm, inside diameter 2.0 cm) as previously described in Thiessen 2010 (Doty, Entzminger et al. 1999; Thiessen, Glazner et al. 2010).

3.4.2 Animal Preparation

The mouse was first weighed. It was then placed in an induction chamber appropriate to the size of the mouse that was connected to an isofluorane vaporizer. Isofluorane (5%) in oxygen/nitrous oxide (30/70) was administered into the induction chamber until the mouse lost its righting reflex. The animal was then removed from the chamber and transferred to a nose cone apparatus where the isofluorane mixture was continued at 1-2% to maintain a deep plane of anesthesia such that the mouse had no response to painful stimuli (toe pinch). Excess isofluorane was removed from the magnet bore by scavenging line. While anesthetized, the mouse was positioned prone on a handmade polyethylene cradle with securing the head in a 2.4-cm inner diameter, modified quadrature birdcage volume coil (NRC-IBD, Winnipeg, MB, Canada). During the experiment, the magnet bore temperature was maintained 32.4-34.0˚C with an extra-flexible PVC-insulated probe

with a PVC-coated tip thermocouple (Cole-Parmer Canada, Anjou, QC, Canada). The respiration rate was monitored using a standard monitoring and gating system (Model 1025, SA Instruments, Inc., Stony Brook, NY, USA) by a respiratory pad placed under the mouse, with an ideal rate of 130/60 bmp.

3.4.3 Imaging Acquisition/ Scanning

The mouse in the RF coil apparatus was positioned in the bore of the MRI machine. A series of scout images were first acquired in order to align the slice of hippocampus to be imaged using the reference point 1 mm rostral to the location of pituitary, which can be easily seen in a FLASH image due to its high signal, see Figure 6.

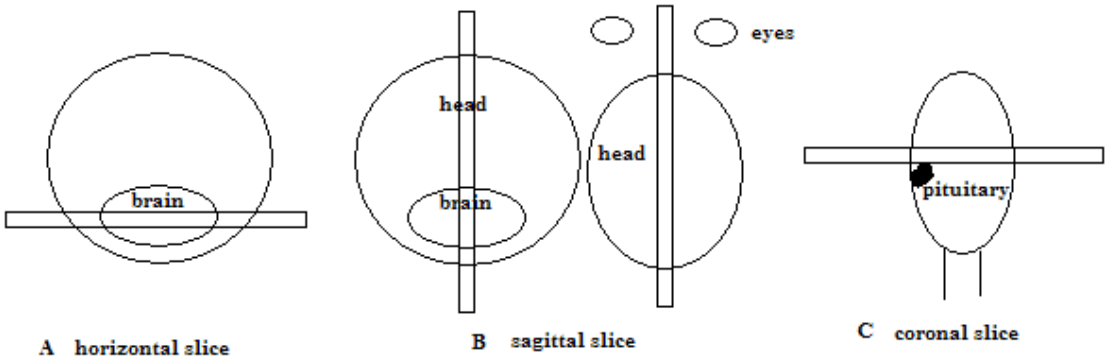

Figure 6 Positioning of magnet to capture image of mouse hippocampus.
(A) Alignment of horizontal slice. (B) Alignment of sagittal slice using the reference location of A. (C) Alignment of coronal slice using the reference location of B and the location of the high signal (bright) pituitary.

Next, high-resolution T2-weighted images were acquired in six 3-months old (3 wild-type & 3 TgCRND8) and six 12-16 months old (3 wild-type and 3 TgCRND8). This was performed using a multi-slice single-echo sequence (MMSE) with five slices 1 mm apart, where the 4^{th} slice was aligned on the pituitary; TR 1540ms, TE 80ms. A field of view

(FOV) of 25 X 25 mm, a matrix of 256 x 256, 98 x 98 µm in-plane resolution, a slice thickness of 0.75 mm, and 16 averages (total scan time 1 h 45 m). Next, diffusion weighted imaging (DWI) was performed on 12-16 month old mice with a magnetization prepared Turbo-FLASH imaging sequence (Thomas, Pell et al. 1998). Two of the controls and one transgenic mouse were imaged with a 30 X 30 mm FOV, while the rest were imaged with a 40 x 40 mm FOV due to heating problems in the gradient coils for a total of 11 mice.

DWI was acquired using the above parameters in three directions; vertical/sagittal (y), horizontal (x) and coronal (z) with a 128 x 128 matrix size, in-plane resolution of 234 x 234 µm or 313 x 313 µm (based on different FOVs), a slice thickness of 1 mm, and 32 averages. Eight DWIs were acquired in each of x, y, and z with varying gradient strengths (gradient pulse duration, δ = 18 ms; gradient pulse separation, Δ = 20 ms; gradient pulse strength, g = 8.0, 16.1, 24.11, 32.2, 40.2, 48.3, 56.3 and 64.4 mT/m) with respective *b* values of 21.0, 84.1, 189.1, 336.3, 525.4, 756.6, 1029.8, and 1345.0 s/mm2 calculated using $b = \gamma^2 g^2 \delta^2 (\Delta - \delta/3)$ – the diffusion-weighted factor equation for symmetric and square gradient pulses (Stejskal and Tanner 1965). Phase shift causes distortion, which was corrected by the quadratic summation of two complementary images at each b value, with the second image having a 90˚ flip-back pulse phase shifted by $\Pi/2$ (Thomas, Pell et al. 1998). Scan time for each set of DWI was 16 m 20 s for a total scan time of 1h38min.

3.4.4 Image Analysis

High-resolution T2-weighted images were enlarged to visualize plaque deposition in the hippocampus and neocortical regions. Diffusion weighted images were used to

calculate apparent diffusion coefficient (ADC) maps using each diffusion direction (ADCx, ADCy, and ADCz) as well as the mean ADC. This was done by applying the Stejskal-Tanner equation ($S = S_0e^{-bADC}$, where S_0 is the signal intensity when b=0, or when no diffusion-weighted gradients are applied) using a custom designed MATLAB code written by Jonathan Thiessen (University of Manitoba, student of Dr. Melanie Martin) (Stejskal and Tanner 1965; Kantarci, Jack et al. 2001; Kantarci, Petersen et al. 2005). From the generated ADC maps, Regions of Interest (ROI) were selected corresponding to the areas of the hippocampus, cerebral cortices, left and right hemispheres and the third ventricle (see Figure 7) with the aid of the MAP mouse brain atlas [http://www.loni.ucla.edu/MAP/] (see Figure 8) and SHIVA visualization software (MacKenzie-Graham, Lee et al. 2004). An average ADC value was calculated for each ROI using MATLAB and statistically analyzed between transgenic TgCRND8 mice and their littermate controls using a two-tailed *t* test.

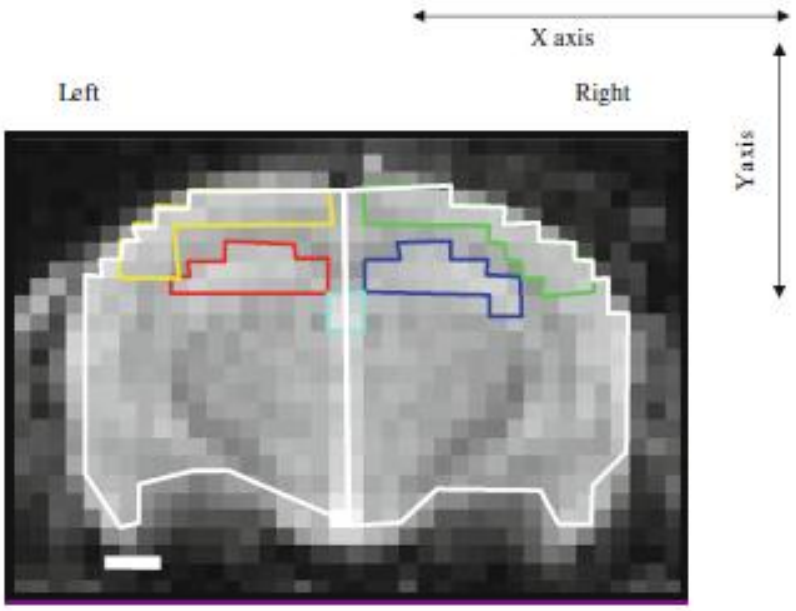

Figure 7 Sample ROI determination for ADC calculations in the hippocampal formation-coronal plane of mouse brain.

Diffusion-weighted images (b=21 s/mm2, x-direction) were used to select the ROIs. The outlines are as follows: yellow – left cerebral cortex, green – right cerebral cortex, red – left hippocampus, blue – right hippocampus, cyan – third ventricle and white – two hemispheres of the brain. Scale bar = 1mm.

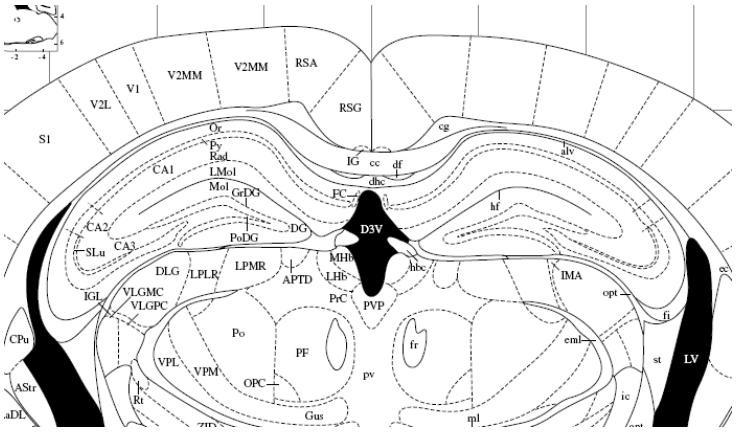

Figure 8 Representation of image from MAP mouse brain atlas.

Source: *http://www.loni.ucla.edu/MAP/*

3.5 Molecular Assays

3.5.1 Quantitative real time polymerase chain reaction (qRT-PCR)

QRT-PCR (performed by Gary Odero – technician- Albensi lab) was used to assay for expression of APP mRNA in the hippocampus of the C3H and 129SvEv transgenic strains at one year of age as previously reported in Glazner 2010 (Glazner, Odero et al. 2010). Samples were normalized to glyceraldehydes-3-phosphate dehydrogenase (GAPDH). Following manufacturer's instructions, total RNA was extracted from frozen hippocampal tissue (3 control and 3 transgenic mice) with the Allprep DNA/RNA/protein Kit (Qiagen, Mississauga, ON, Canada). A sample of 200 ng of RNA was used to synthesize cDNA with the iScript cDNA Synthesis Kit (BioRad) following manufacturer's instructions. APP, IDE and GAPDH were amplified with the primers listed in Table 1 and confirmed by gel electrophoresis.

Table 1 - Primer Pairs for qRT-PCR.

Gene	Primer Sequence (5' to 3')	PCR product size (bp)	Tm (˚C)	Primer Conc. (µM)
IDE	CGG CCA TCC AGA GAA TAG AA TTT GGA GGC TCT GAC AGT GA	193	64.5	1.0
APP	GCA GAA TGG AAA ATG GGA GTC AAT CAC GAT GTG GGT CTG CGT C	199	62	0.75
GAPDH	CGT GTT CCT ACC CCC AAT GTG TCC CTC AGA TGC CTG CTT CAC CAC CTT C	102	69.4	1.0

To ensure no gDNA contamination, RNA was used as a negative control. PCR cycles consist of 94˚C for 2 minutes (1 cycle), 94˚C for 30 seconds, 64.5˚C for 30 seconds, 72˚C for 1 minute (40 cycles); 72˚C for 7 minutes (1 cycle); hold at 4˚C. PCR products were purified using the GenElute PCR Clean-up Kit (Sigma Aldrich). Standard curves for this experiment were created with serial dilutions of the PCR products from both genes (APP and IDE). Quantitative PCR was then performed using a Bio-Rad iCycler Thermal Cycler with iQSYBR Green Super Mix (BIORAD). A total of 2 µl of cDNA was used for all experiments. All experiments were performed in triplicate. Copy number for APP and IDE were calculated from the standard curve. Quantitative real-time-PCR conditions were: 98˚C for 30 seconds, 95˚C for 5 seconds, 64.5˚C for 15 seconds, 72˚C for 15 seconds, 80˚C for 10 seconds (40 cycles), 72˚C for 60 seconds, 95˚C for 60 seconds, 95˚C for 10 seconds and hold at 4˚C.

4. RESULTS

4.1. General Observations

Obvious behavioral differences among groups, based on background, while housed in their home cages were not observed. However, the animal facility staff noted that the males of both background strains fought more than their female counterparts. The females were typically housed with 3-5 per cage, while the males slightly less. We found a 25% mortality rate in animals 6 months or older, similar to that found in other labs (personal communication). This rate was equivalent between all groups.

4.2 Effect of different background strain on behavior

Background strain did affect behavior as previously reported in Glazner 2010.

4.2.1 Escape latency

In the acquisition phase, both the C3H/C57F1 and 129SvEvtac/C57F1 transgenic mice had significantly longer escape latencies (Figure 9 top & bottom) over the 7 day period than their respective littermate controls (ANOVA: C3H/C57F1, $p = 0.0145$; 129SvEvtac/C57F1, $p = 0.00134$) . Also, it appeared that the 129SvEv transgenic mice had severely impaired learning as there was no obvious decrease in the escape latency times over the seven day acquisition phase (Figure 9 bottom) in contrast to the gradual decrease in escape latency times for the C3H transgenic strain (Figure 9 top). One might wonder whether this may be attributable to a difference in swim ability between the two background strains. However, we found identical swim speeds (data not shown –

calculated by Anna Motnenko – summer student – Albensi lab) suggesting no overt motor deficits, or an impaired ability to swim.

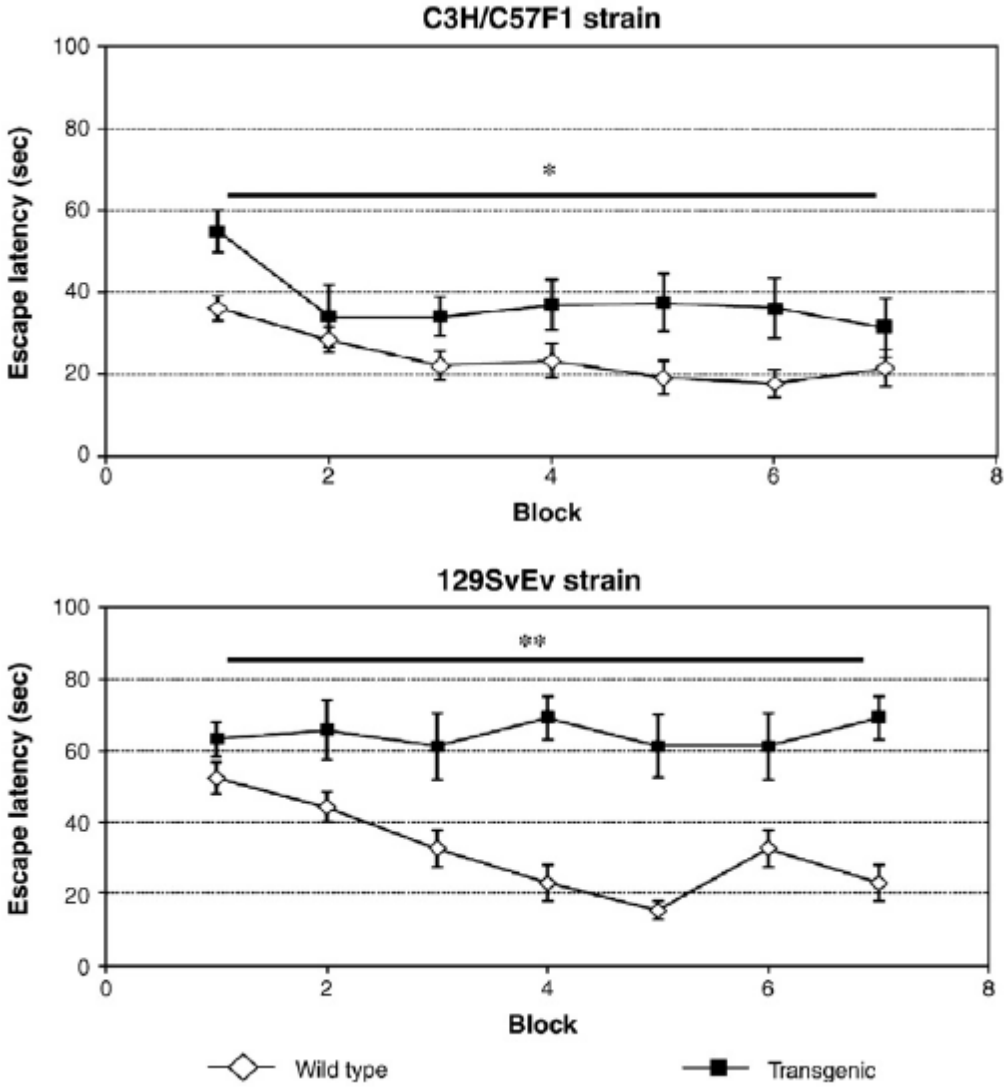

Figure 9 - Escape Latency.
Times were recorded over seven blocks of the acquisition phase of the MWM. C3H and 129SvEv one-year-old transgenic mice had significantly longer escape latencies than their respective age-matched littermate controls (C3H, *p = 0.0145, F = 7.17; 129SvEv **p = 0.00134, F = 15.03). Error bars represent +/- SEMs. N = 10 each.

4.2.2. Search strategy

It was expected that with each subsequent daily exposure in the water maze, each trial would show an increase in the use of spatial strategies as the animal encodes a spatial map of the maze. This was in fact observed for both littermates of the C3H and 129SvEv backgrounds (Figure 10A) with each using spatial strategies 71.8% and 62.1% of the time, respectively. The remainder of littermate search strategies was non-spatial systematic (21% vs. 36.1%) and repetitive looping (7.1% vs. 1.7%) for the C3H versus 129SvEv strains. In contrast, the C3H transgenic mice used spatial (43.3%), non-spatial systematic (48.2%), and repetitive looping (8.3%) strategies, respectively. The 129SvEv mice showed a mixture of all three-search strategies (32.4% spatial, 36.8% non-spatial systematic, and 31.2% repetitive looping), demonstrating the greatest memory impairment. The 129SvEv seemed to not have a preference for any search strategy.

As expected, both transgenic background strains showed significantly lower incidents of spatial search strategies compared to their respective littermate controls ($p = 0.0013$ C3H, and $p = 0.0179$ 129SvEv) (Figure 10B). The C3H transgenic mice showed an increase in the use of non-spatial search strategies ($p = 0.0018$) as the acquisition phase progressed, as compared to their littermate controls, suggesting a transition from spatial to non-spatial systematic strategies. Lastly, the repetitive looping strategy was used significantly more by transgenic 129SvEv versus their littermate controls ($p < 0.05$), significantly less by 129SvEv controls versus C3H controls ($p < 0.05$), and significantly more by 129SvEv transgenic mice versus C3H transgenic mice ($p < 0.05$) (Figure 10B).

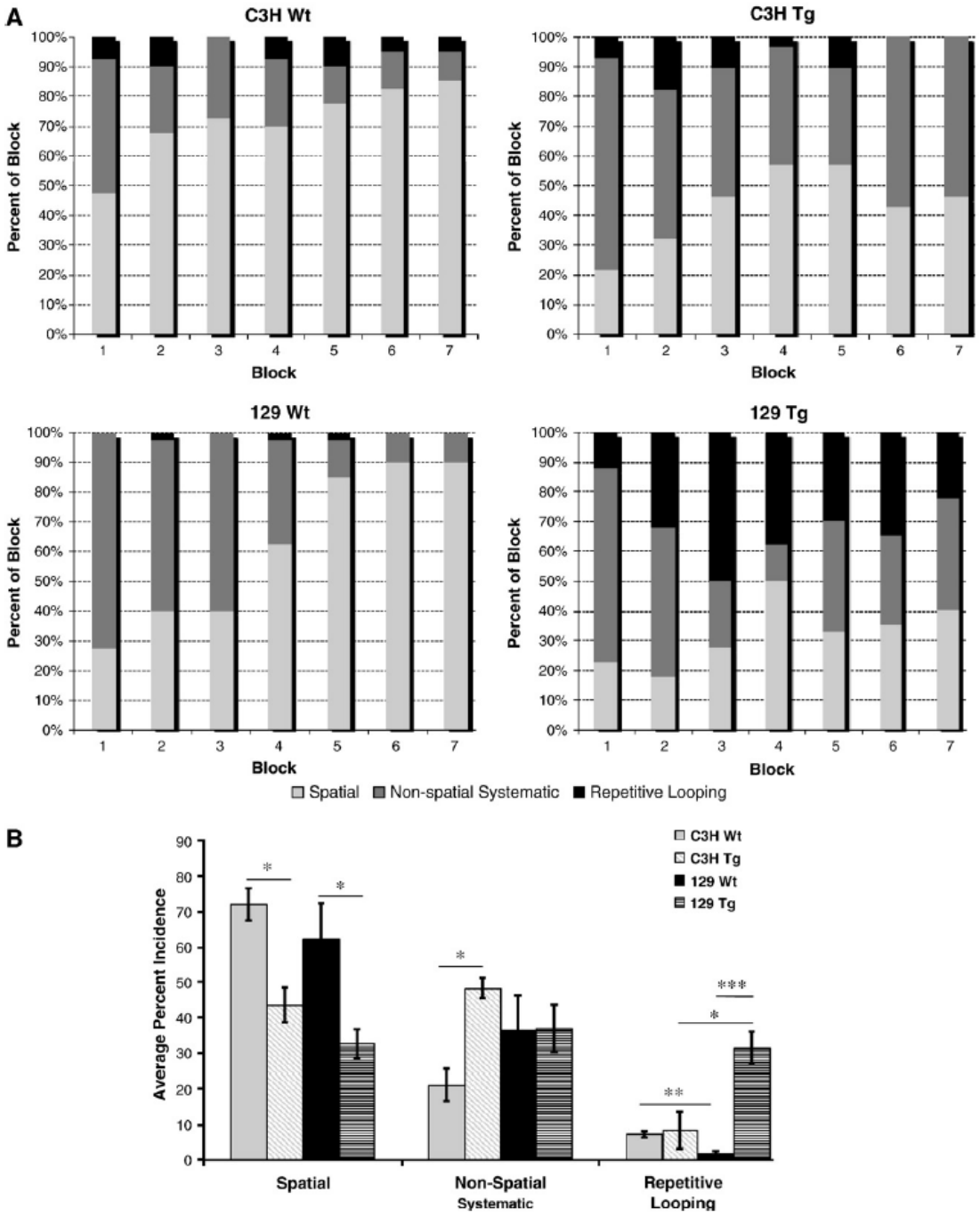

Figure 10 - Search Strategies in the Morris water maze.
(A) Search strategies for 1-year-old C3H and 129SvEv background strains. (B) Quantification of search strategies. Search strategies were assigned during the seven day acquisition phase. Quantification was accomplished by averaging each search strategy category over the course of the entire acquisition phase. Error bars represent +/- SEMs. *$p < 0.05$, **$p < 0.01$ and ***$p < 0.001$. Graphs generated by G. Odero. N = 10 each.

4.2.3 Swim path length.

While each mouse regardless of genetic makeup followed a different path in each acquisition trial, representative traces of swim path are shown in Figure 11A.

For path length, the 129SvEv transgenic mice demonstrated a significant increase ($p = 0.017$) in the average distance they swam before they successfully found the location of the hidden platform, thus suggesting impairment in the ability to recall the position of the platform as they took longer to find the platform (Figure 11B). Despite the impairments witnessed in with Escape Latency and Search Strategy measurements, no significant difference ($p>0.05$) in average path length was observed in the C3H/C57F1 strain. This suggests that background strain does differentially affect the acquisition of spatial memory in the TgCRND8 mice.

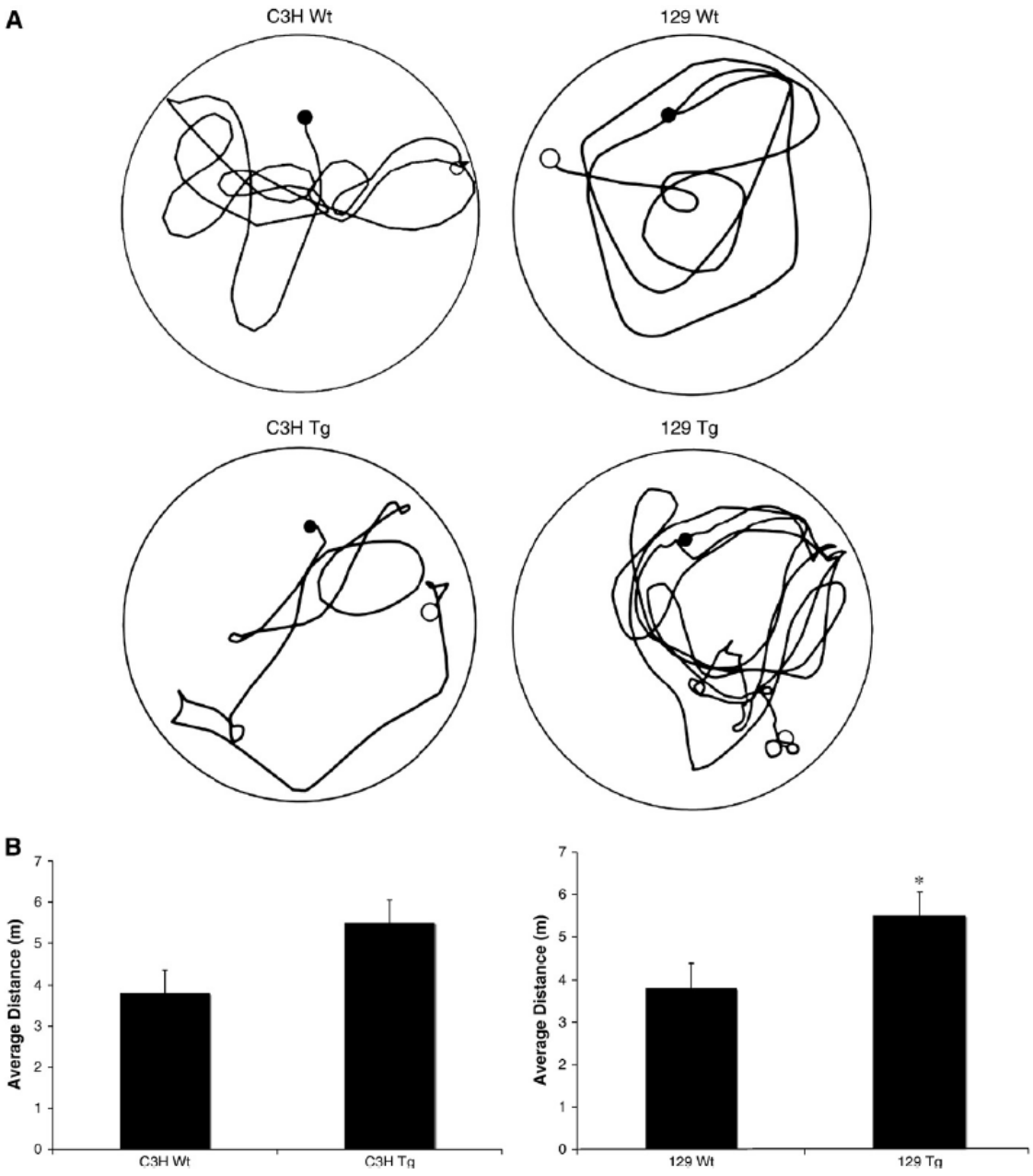

Figure 11 - Acquisition phase in year old C3H and 129SvEv strains.
(A) Representative traces of swim path. (B) Average path lengths. Closed circles indicate the position of the hidden platform and open circles are the position of mouse entry into the testing pool. The average path length represents the average distance swam over the entire seven day acquisition phase. Error bars represent +/- SEMs. *$p<0.05$. Graph generated by Anna Motnenko. N = 10 each.

4.2.4 Time in Target Quadrant

The time in the correct target quadrant (having had the removed platform) was recorded over the three days of the retention phase. There was no difference between either background strain (C3H/C57F1 p=0.653 and 129SvEvtac/C57F1 p=0.833).

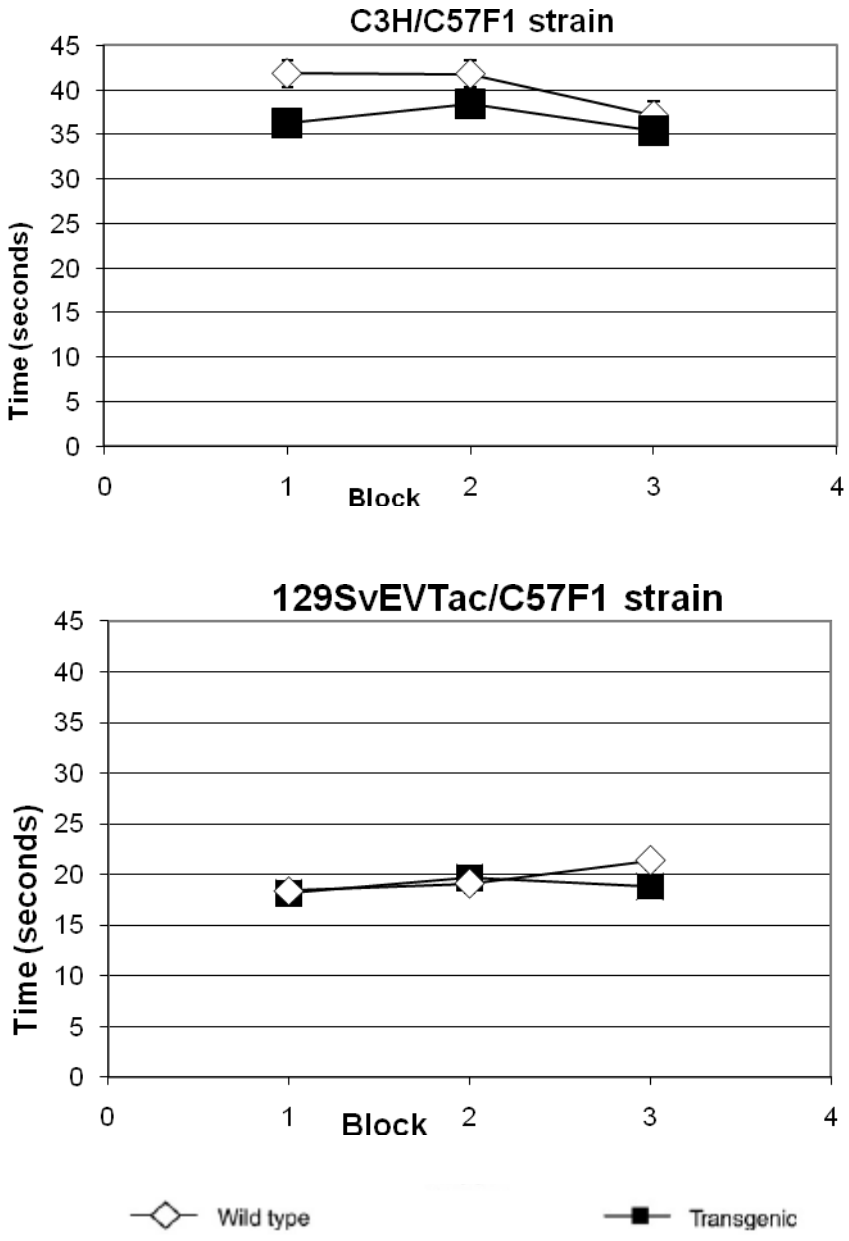

Figure 12 - Time in Correct Target Quadrant.
Error bars represent +/- SEM. N = 10 each.

4.2.5 Number of passes over removed platform

The number of passes over the location of the target (that was removed) was recorded over the three days of the retention phase. There was no difference observed in the number of passes for either background strain (C3H/C57F1 p=0.330 and 129SvEvtac/C57F1 p=0.714).

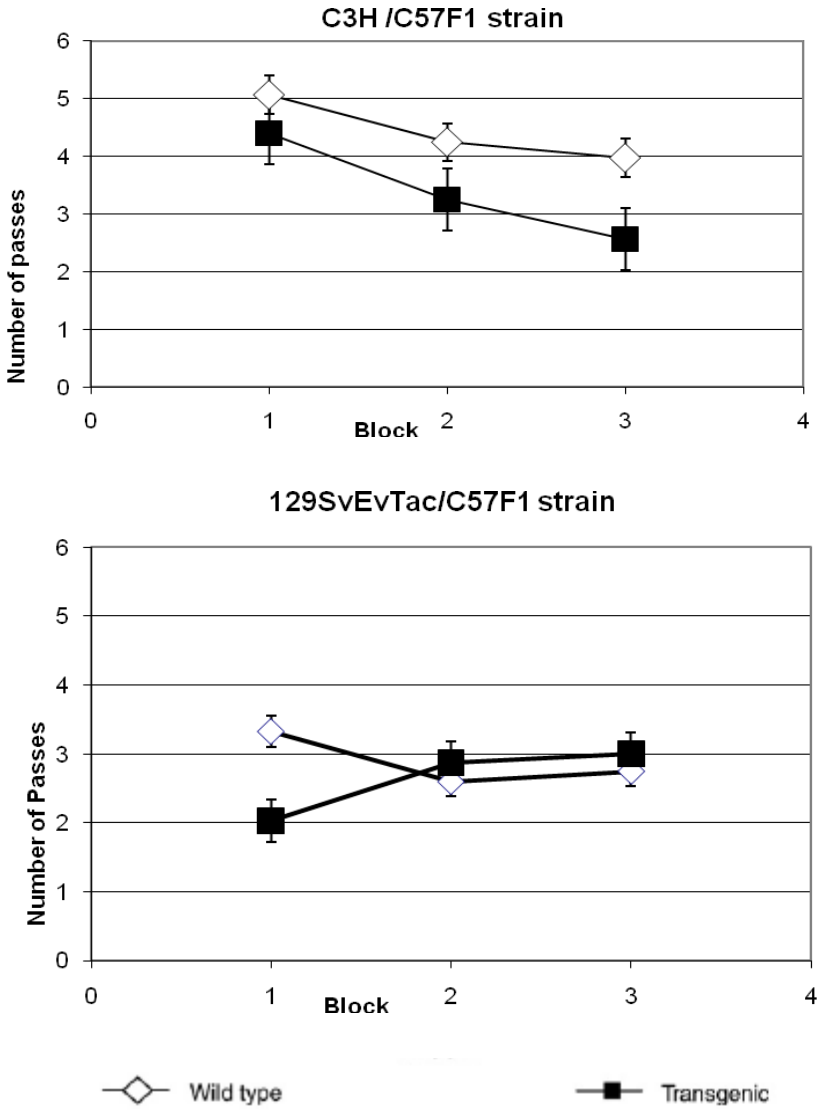

Figure 13 - Number of Passes.
Error bars represent +/- SEM. N = 10 each.

4.2.6 Annulus Crossing Index

The ACI demonstrated that the C3H CRND8 transgenic mice showed impairment as compared to their controls (p=0.012) while those on the 129SvEv background did not show this impairment (p=0.930). However, these findings may be attributed to the C3H controls learning a spatial map better than the 129SvEv controls, rather than a difference attributable to transgene insertion, see Figure 14. Data was pooled for gender. (C3H: p=0.76, 129SvEv p=0.68).

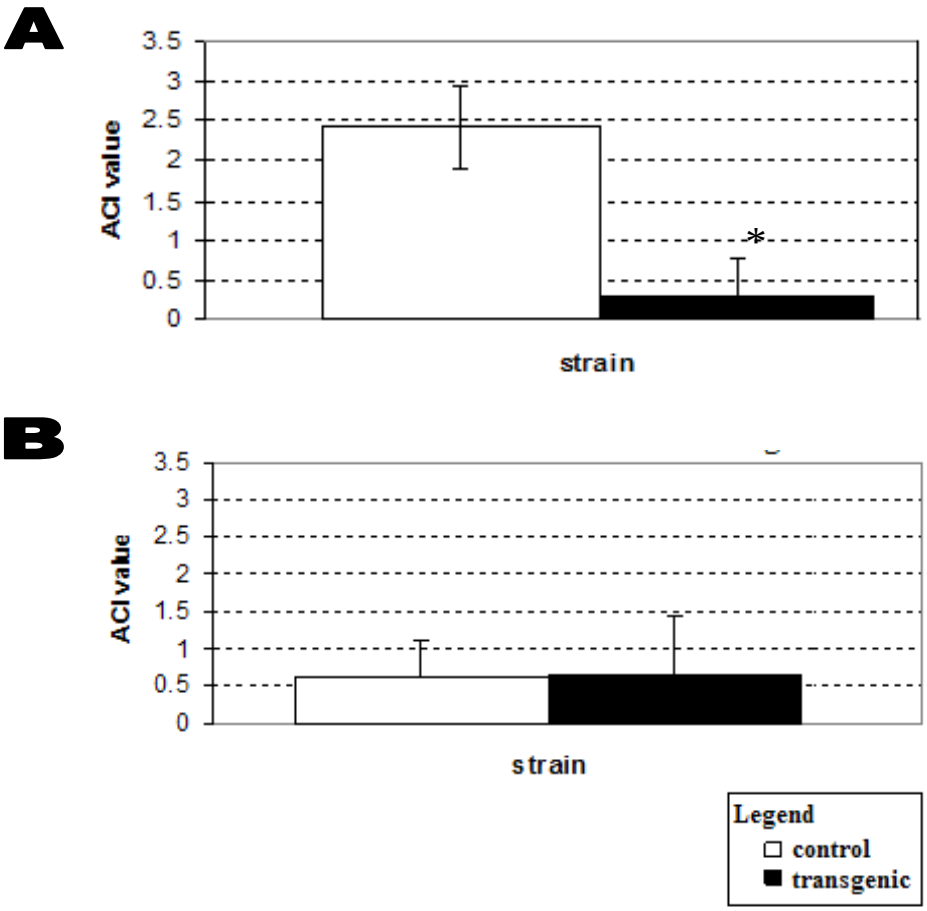

Figure 14 - Annulus Crossing Index.
Controls vs transgenic mice in the Retention Phase of the Morris water maze. (A) C3H/C57F1 background strain (B) 129SvEvtac/C57F1 background strain. N = 10 each.

4.3 Magnetic Resonance Imaging

4.3.1 High Resolution T2-weighted images

High-resolution T2-weighted images of control and TgCRND8 at one year of age were compared for potential anatomical differences. One feature, a hypointense line in the CA1 region of the hippocampus (see red arrow in Figure 15), was more prominent in the littermate than transgenic at one year of age.

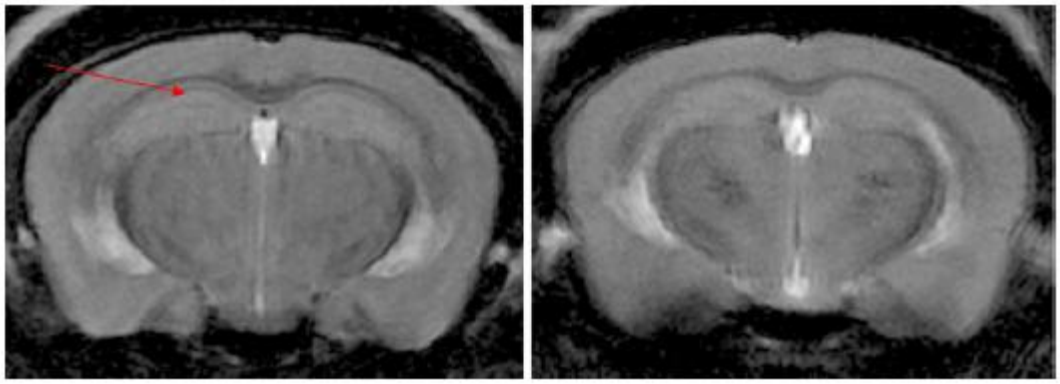

Figure 15 - Representative Images from in-vivo T2-weighted coronal scans of normal CRND8 wildtype (left) versus TgCRND8 (right).
The red arrow indicates the CA1 pyramidal cell layer, which appears to be lost in the transgenic mouse, scan (n=3 for each).

To further explore this observation, an *ex vivo* T2-weighted scan was performed in a custom made apparatus which held one hemisphere of control CRND8 brain and one hemisphere of transgenic CRND8 brain side by side as seen in Figure 16.

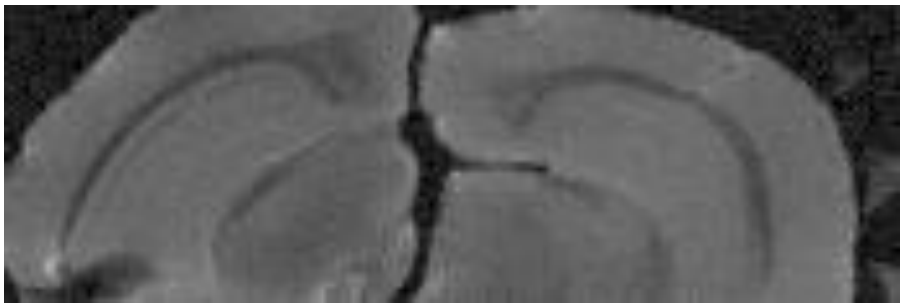

Figure 16 - Ex-vivo T2-weighted coronal scans of normal CRND8 wildtype (left) and TgCRND8 (right).
Each brain was bisected into two hemispheres and one half placed in the custom holder. The brains were imaged with the same parameters as the in-vivo T2-weighted scans. (n=1).

When analyzing the 3-month old control CRND8, this hypointense line was not as prominent as in the 1-year-old control mice, and it was barely visible in the TgCRND8 mice at 3 months. This observation had unclear significance as there was no visible difference in histological sections where all four groups showed a normal CA1 pyramidal cell body layer (see Figure 18 – orange arrows).

4.3.2 Diffusion Weighted Images

A total of 11 animals (4 wildtype and 7 TgCRND8) between 12-16 months were used to calculate ADC values from ROIs within hippocampal and neocortical regions. No significant differences in ADC values were found between control littermate mice and their transgenic counterpart ($p > 0.05$) (Table 2).

Table 2 - Mean ADC values (x10-4 mm2/s) for 12-16 month old mice.
The colors (red, blue, yellow, green and white) correspond to the outlines as seen in Figure 7.

Regions of interest	Wild type ($n = 4$)	CRND8 transgenic ($n = 7$)
Hippocampus (left), red	8.57 ± 0.38	8.09 ± 0.29
Hippocampus (right), blue	8.40 ± 0.20	8.02 ± 0.30
Hippocampus (combined), red + blue	8.50 ± 0.30	8.05 ± 0.28
Cerebral cortex (left), yellow	8.19 ± 0.57	7.42 ± 0.21
Cerebral cortex (right), green	7.93 ± 0.37	7.52 ± 0.27
Cerebral cortex (combined), yellow + green	8.06 ± 0.47	7.49 ± 0.21
Left hemisphere, white	8.57 ± 0.38	8.09 ± 0.29
Right hemisphere, white	8.40 ± 0.20	8.02 ± 0.30
Whole brain (all)	8.50 ± 0.30	8.05 ± 0.28

Data are presented as mean ± SEM

4.4 Histology

4.4.1 One year old mice from different background strains used in Behavioral Studies

To explore the discrepancy in the ability to form hippocampal dependent spatial memory in the MWM, we next attempted to visualize and quantify Aβ plaque burden in this brain region. Thioflavin S staining of coronal sample slices showed robust amyloid beta plaque deposition in transgenic mouse hippocampi regardless of genetic background strain (Figure 17A). There was no plaque deposition in either control tissue (data not shown). Quantification (Figure 17B) using our custom MatLab software program revealed a significantly higher deposition of amyloid beta plaques in the transgenic 129SvEv mice than their C3H counterparts ($p<0.01$). This data taken together with the decreased performance of the transgenic 129SvEv mice in the MWM suggests that the increased deposition of the Aβ plaque may be related to the observed behavioral

impairment. This suggests that genetic differences in background strains differentially affect the deposition of Aβ in the mouse hippocampus.

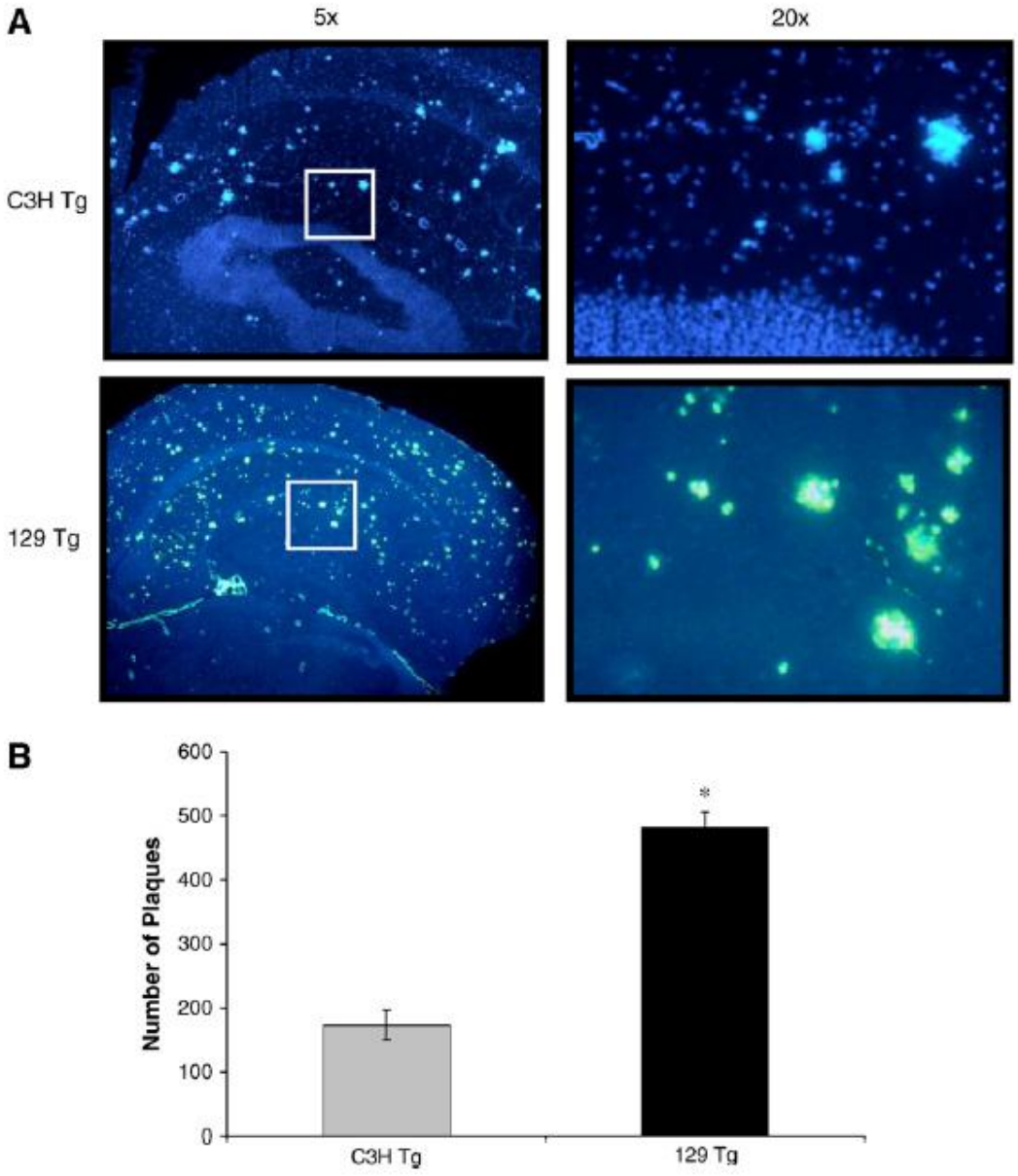

Figure 17 - Fluorescent staining to determine amyloid beta plaque deposition in year old C3H and 129SvEv transgenic mice.
(A) Images of Fluorescent staining for amyloid beta plaques. (B) Number of Plaques. Nuclei were stained with DAPI (blue) and amyloid beta plaques with Thioflavin S (apple green). The number of plaques was determined with a custom MatLab software program. Error bars represent +/- SEMs. *$p<0.05$. N = 2 mice each.

4.4.2 Young and Old Mice post MRI

All mouse brain histology slides were doubly stained with DAPI to stain the nucleus of the cells, thus allowing us to identify the granule cell layer of the dentate gyrus region of the hippocampus, and Congo Red to visualize Aβ plaques. All wild-type mice, both at 3 months and one year, did not produce amyloid beta plaques as shown in Figure 18 A & C. It was only in the older animals that the TgCRND8 mice demonstrated a significant plaque burden, both in number and in size (Figure 18 D).

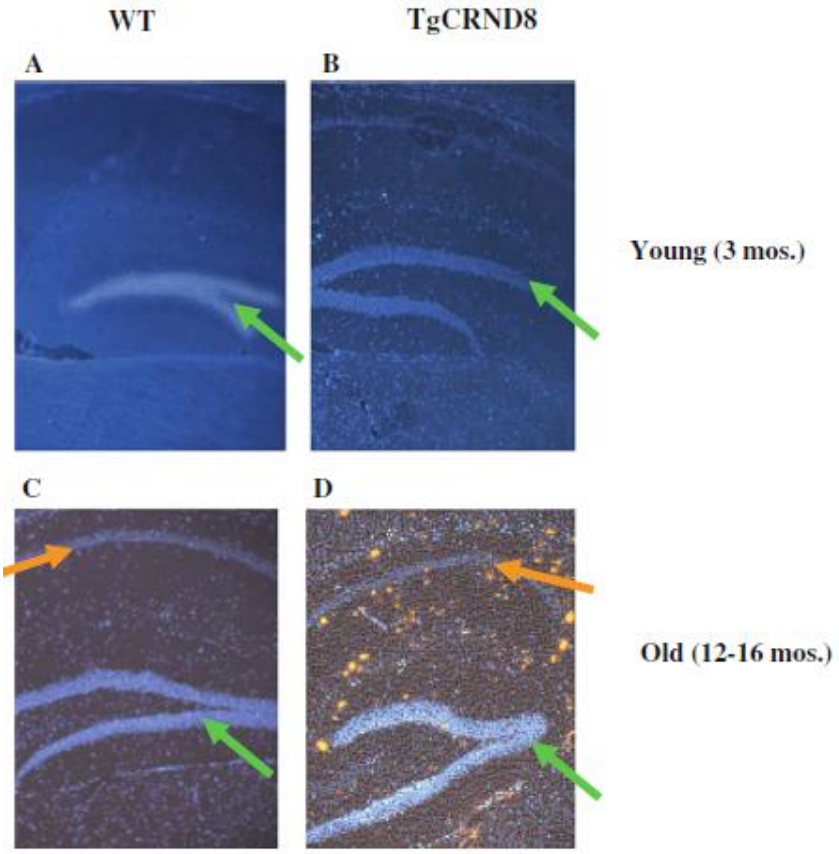

Figure 18 - Representative comparison between littermates (WT) and transgenic CRND8 mice at 3 months (A & B) and one year (C & D).
Brain slices were stained with Congo Red turning amyloid beta orange/red (only visible in older transgenic animals). The green arrows point to the granule cell body layer of the dentate gyrus subfield in the hippocampus. The orange arrows demark the CA1 pyramidal cell body layer and show no obvious difference in appearance between older wildtype and transgenic sections. Magnification: approximately 5X. N = 2 mice each.

4.5 Molecular Assays

4.5.1 Quantitative real-time PCR of APP

To investigate if differences in levels of transgene expression existed between the two transgenic strains, qRT-PCR was used to assay for APP. This data showed a significant, but small, ~10% decrease ($p<0.05$) in the expression of APP mRNA in the 129SvEvtac/C57F1 as compared to the C3H/C57F1 as seen in Figure 19.

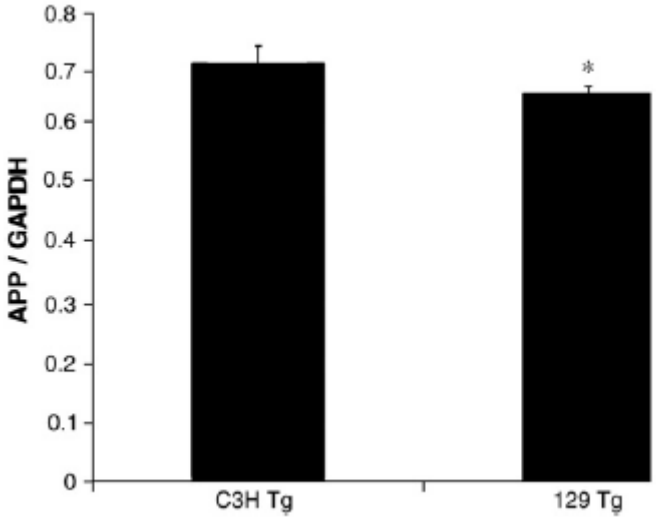

Figure 19 - Quantitative real-time PCR for APP in 1 year old C3H and 129SvEv transgenic strains.
Experiment was performed using qRT-PCR cDNA from whole hippocampal extracts to show the relative expression of APP mRNA. All samples were normalized to GAPDH. *p <0.05. Error bars represent +/- SEMs. N = 3 for C3H and 129SvEv.

4.5.2 Quantitative real-time PCR of IDE

To assess if Aβ clearance, which may influence plaque burden, was different in the two strains, we used quantitative real-time (qRT)-PCR to assay for insulin degrading enzyme (IDE), an important Aβ clearance protein. qRT-PCR showed a significant

decrease in the IDE mRNA expression in the 129SvEvtac/C57F1 stain as compared to the C3H/C57F1 strain ($p = 0.02$) as seen in Figure 20. This suggests that dysfunctional clearance of Aβ is a potential mechanism for the increased plaque burden of the transgenic 129SvEvtac/C57F1 mice.

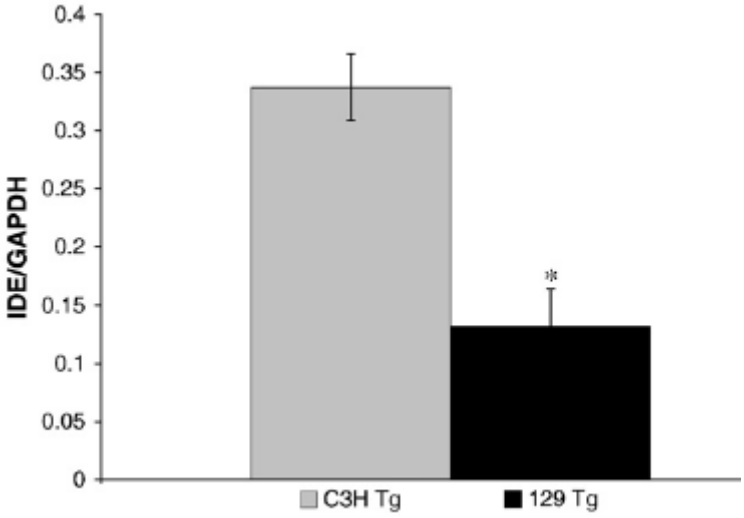

Figure 20 - Quantitative real-time PCR for IDE in 1 year old C3H and 129SvEv transgenic strains.
Experiment was performed using qRT-PCR cDNA from whole hippocampal extracts to show the relative expression of IDE mRNA. All samples were normalized to GAPDH. *p <0.05. Error bars represent +/- SEMs. N= 3 for C3H and 129SvEv.

5. DISCUSSION

The goal of these experiments was to determine if, and to what extent, mouse background strain (129SvEvtac/C57F1 and C3H/C57F1) affected the genotypic and phenotypic expression of the AD-linked mutant APP gene. To accomplish this, we studied mutant APP expression, plaque load, IDE expression, and learning/memory ability in two strains of mice both expressing the 'Swedish' KM670/671NL + V717F 'Indiana' mutation. The results indicate that background strain has a significant effect on phenotypic, but not genotypic, expression of the APP gene, while gender had no significant effect on either measure**.**

Our results broadly agree with previously published data, confirming plaque deposition and loss of cognitive function. However, since we did not carefully perform an age-dependent study, we do not know if the strain-dependent variations we observed at one year were due to differences in 'age of onset' between the strains.

In finding differences in phenotypic impact of mutant genes in different strains, a primary contributing factor would be differences in gene expression. Multiple variables, including number of gene copies inserted and points of insertion, can render transgenes more or less effective, due to deviation in production of the protein of interest. In this study, however, we found no significant variation in mRNA for mutant APP, indicating both strains showed equal gene expression. This is a critical observation, as variations between strains in this parameter would almost certainly be due to experimental (i.e. generation of the transgenic animal) variation, and not some other physiological factor, which would be of clinical and scientific interest. Therefore, downstream consequences

of this gene expression, and any variation seen between groups, are likely due to physiological or genetic differences between the groups, which are clinically relevant.

In the pathway of amyloidosis, downstream of mAPP expression is plaque formation, which we determined to be different between the two strains backgrounds. Mice from 129SvEvtac/C57F1 background displayed significantly greater plaque load relative to the C3H/C57F1 background at one year of age.

Historically, plaque deposition has been considered a hallmark of AD, and suspected to play a major role in disease development and progression. AD brains generally contain significantly greater plaque load than non-AD brains. Mutations which cause familial AD also cause earlier and greater formation of amyloid plaques than is seen in the general population, and there are measureable indications of inflammation and neuronal death surrounding plaques. However, more recent findings hint that plaques are not directly causative of cognitive decline, but are merely an indicator of Aβ load. Recently, the role of toxic amyloid oligomers, which form plaques at high concentrations, has been implicated as a more likely cause of neuronal toxicity. Nevertheless, plaque load does correlate well with cognitive decline (in humans and in animal models) and neuronal death (in humans), thus it remains an important measure of neuropathology.

The two opposing pathways of production and degradation can influence the amount of amyloidogenic Aβ1-42 most directly. One of the primary enzymes responsible for Aβ degradation is IDE. We found that 129SvEvtac/C57F1 mouse brain contained significantly less IDE mRNA compared to those from C3H/C57F1 background, inversely correlated with results of plaque load. Brains from AD patients demonstrate significantly reduced levels of IDE (Perez, Morelli et al. 2000; Cook, Leverenz et al. 2003). In mice

containing AD-linked human genes, inhibition of IDE causes elevated Aβ, while enhancement of IDE results in decreased Aβ (McDermott and Gibson 1997; Farris, Mansourian et al. 2003; Miller, Eckman et al. 2003). Therefore IDE appears to be a significant factor influencing Aβ levels, and would be consistent with the reduced amyloid plaque load we observed in C3H/C57F1 relative to 129SvEvtac/C57F1 brains.

The most clinically relevant endpoint of the TgCRND8 model is cognitive decline, as this demonstrates the neurotoxicity associated with Aβ. Using the Morris water maze as our paradigm, we determined several measures of cognition and, as in plaque load and IDE expression, there were significant differences between the two strains. The 129SvEvtac/C57F1 required significantly greater time to find the hidden platform after training, than did C3H/C57F1. In fact, the latter strain needed only slightly more than half the time as the former, a striking difference in background strains given the equivalence of mAPP gene expression between the two. This result is correlated with plaque load between the two strains, in which higher plaque load is associated with reduced cognitive ability, and thus supports the contention that plaque load in this model is a good indicator of clinically-relevant behavioral pathology.

A more detailed analysis of MWM performance was conducted in order to reveal search strategies. Here we observed that TgC3H/C57F1 used spatial systemic strategies, while the slower-learning Tg129SvEvtac/C57F1 showed no significant preference for any of the strategies tested. Hippocampal function is critical to spatial learning, and the formation of a spatial map by the hippocampus is thought to underlie success in spatial tasks such as the MWM (Tolman 1948; Amsel 1993). Although not conclusively determined, spatial strategies are widely thought to represent a greater level of cognition

and learning ability because by using learned or remembered cues, the animal quickly narrows the search to the correct quadrant (Morris 1984; Brody and Holtzman 2006). Non-spatial strategies, on the other hand, may indicate a more random and imprecise pattern, in which prior experience in the maze is not used to guide the animal (Janus 2004). Both strains demonstrated an increase in use of spatial strategies over the course of the testing, indicating the ability to learn and remember, or in other words to form a spatial map for later retrieval when subsequently challenged with the MWM. The greater usage of this strategy by the TgC3H/C57F1 strain, which required less time to find the platform, supports the idea that spatial strategies are indicative of a greater ability to learn, and also that this strain suffered less cognitive decline than did the Tg129SvEvtac/C57F1 strain.

Our observed results follow previous reports showing strain-dependent variations in transgene- linked neuropathy. Chishti et al. 2001 showed that crossbreeding TgCRND8 mice from FVB or 129SvEvtac with C3H/C57F1 increased survival. More recently, it is was reported in TgCRND8 transgenic animals that both Aβ plaque load and animal survival differed between the B6 and A/J background strain (Sebastiani, Krzywkowski et al. 2006). These reports support our contention that relatively small differences in strains can have a major impact on pathology associated with disease-linked transgenes. This raises the possibility that we can exploit these strain differences in order to find potentially critical, previously unknown genetic susceptibility factors.

Sporadic AD accounts for >95% of all cases, and as opposed to familial AD; we still do not know the factors which determine susceptibility. As discussed in the introduction, there have been numerous genetic and environmental risk factors identified, but (except

for Apoε4) the relative increase in risk from any of these is minor. Animal models, though not true models of human AD, allow us to reduce the 'noise' from environmental effects and focus on potential genetic factors. If two closely related strains of mice, expressing equivalent levels of transgene, display significantly different severity of neuropathy, then this strongly suggests that relatively minor genetic factors may play a critical role in disease development. In our study, we demonstrated a significant difference in expression of IDE, while others have shown strain-dependent variations in levels or phosphorylation of other proteins relevant to AD such as CREB, Egr-1, c-Src, and CaMKII (Patil, Schlick et al. 2009). We may be able to exploit the differences in strain susceptibility to find other genetic risk factors.

Some substrains of the 129SvEvtac/C57F1 background have measurable histological defects in the corpus callosum, which is critical to cognition and is damaged in AD regions (Wahlsten 1982). Thus, relatively minor genetic variations may result in measureable neuroanatomical features, which may be mimicked in humans. Thus anatomical strain variations may point us to useful parameters in which to determine who is at greater risk for development of AD. Most environmental (life habits, supplements, etc) factors shown to reduce risk of *development* of AD show essentially no effect on disease *progression* in AD patients. In addition, drugs that improve function in AD patients tend to be most effective early in the disease. Therefore, for both the potential to reduce development of AD and for the improved efficacy of drugs, determining who is 'most at risk' would be a significant advance in the field. Currently, not only can we not effectively assess AD risk, but we cannot even determine with certitude that a patient

even has AD until after death. Clearly, exploiting strain differences to determine biochemical and anatomical risk factors and risk features is an important future goal.

6. FUTURE DIRECTIONS

The pathway of toxic amyloidosis modeled by the TgCRND8 transgenic animal proceeds from the starting point of an overexpression of mutant human APP, to production of monomeric amyloidogenic $A\beta_{1-42}$ and then formation of soluble and then insoluble Aβ oligomers. This results in endpoints of amyloid plaques and cognitive decline. Though we have demonstrated equivalent mRNA for hAPP with differences in plaque load, IDE expression, and cognition as measured by MWM, there are clear gaps that need to be addressed. We measured mRNA for hAPP, demonstrating equivalent transgene insertion; we did not measure protein levels of APP, which is the critical substrate for Aβ production. Of even greater importance would be direct determination of Aβ-42 levels, which are regulated by numerous pathways including IDE.

Determination that Aβ levels are indeed decreased in TgC3H/C57F1 would support our hypothesis that IDE may play a role in decreased plaque formation and increased cognitive ability, while the opposite result would require a re-examination of our hypothesis and a search for differences in the biochemical pathway downstream of Aβ-42 production/degradation. In addition, it would be of great interest to determine if the dichotomy in disease severity is age-dependent, and thus a time course of effect would be interesting.

Generally, as mentioned, the true strength of this kind of study is that it provides a model of the role epigenetics and relatively minor genetic differences may play in disease development and progression in the face of a potent disease-inducing mutation such as that found in the TgCRND8 model. The ultimate goal of medical research is to

understand disease states in order to find effective strategies for treating, and hopefully in time curing the pathology. Studies such as this may be used as a starting point to identify, using techniques unavailable until recently, genetic and epigenetic risk factors for sporadic AD, which could then be used to develop clinical treatments for AD.

APPENDIX

Additional Mouse Information

Table 3 - Information about CRND8 mice

ID	Sex	Genotype	Age (months)	Breeding Site
33025	F	Tg(swe+V717F)8 -/- (129SvEvtac/C57F1)	12	CRND
33026	F	Tg(swe+V717F)8 -/- (129SvEvtac/C57F1)	12	CRND
33052	F	Tg(swe+V717F)8 -/- (129SvEvtac/C57F1)	12	CRND
33181	F	Tg(swe+V717F)8 -/- (129SvEvtac/C57F1)	12	CRND
33185	F	Tg(swe+V717F)8 -/- (129SvEvtac/C57F1)	12	CRND
32604	M	Tg(swe+V717F)8 -/- (129SvEvtac/C57F1)	12	CRND
33012	M	Tg(swe+V717F)8 -/- (129SvEvtac/C57F1)	12	CRND
33013	M	Tg(swe+V717F)8 -/- (129SvEvtac/C57F1)	12	CRND
33272	M	Tg(swe+V717F)8 -/- (129SvEvtac/C57F1)	12	CRND
33278	M	Tg(swe+V717F)8 -/- (129SvEvtac/C57F1)	12	CRND
33050	F	Tg(swe+V717F)8 +/- (129SvEvtac/C57F1)	12	CRND
33051	F	Tg(swe+V717F)8 +/- (129SvEvtac/C57F1)	12	CRND
33053	F	Tg(swe+V717F)8 +/- (129SvEvtac/C57F1)	12	CRND
33054	F	Tg(swe+V717F)8 +/- (129SvEvtac/C57F1)	12	CRND
33055	F	Tg(swe+V717F)8 +/- (129SvEvtac/C57F1)	12	CRND
33186	F	Tg(swe+V717F)8 +/- (129SvEvtac/C57F1)	12	CRND
33187	F	Tg(swe+V717F)8 +/- (129SvEvtac/C57F1)	12	CRND
32603	M	Tg(swe+V717F)8 +/- (129SvEvtac/C57F1)	12	CRND
33271	M	Tg(swe+V717F)8 +/- (129SvEvtac/C57F1)	12	CRND
33280	M	Tg(swe+V717F)8 +/- (129SvEvtac/C57F1)	12	CRND
34207	F	Tg(swe+V717F)8 -/- (C3H/C57F1)	12	CRND
34208	F	Tg(swe+V717F)8 -/- (C3H/C57F1)	12	CRND
1442	F	Tg(swe+V717F)8 -/- (C3H/C57F1)	12	SBRC
1348	F	Tg(swe+V717F)8 -/- (C3H/C57F1)	12	SBRC
1391	F	Tg(swe+V717F)8 -/- (C3H/C57F1)	12	SBRC
34175	M	Tg(swe+V717F)8 -/- (C3H/C57F1)	12	CRND
34403	M	Tg(swe+V717F)8 -/- (C3H/C57F1)	12	CRND
230	M	Tg(swe+V717F)8 -/- (C3H/C57F1)	12	SBRC
34398	F	Tg(swe+V717F)8 +/- (C3H/C57F1)	12	CRND
34399	F	Tg(swe+V717F)8 +/- (C3H/C57F1)	12	CRND
34400	F	Tg(swe+V717F)8 +/- (C3H/C57F1)	12	CRND
224	F	Tg(swe+V717F)8 +/- (C3H/C57F1)	12	SBRC
34402	M	Tg(swe+V717F)8 +/- (C3H/C57F1)	12	CRND
1368	M	Tg(swe+V717F)8 +/- (C3H/C57F1)	12	SBRC
1423	M	Tg(swe+V717F)8 +/- (C3H/C57F1)	12	SBRC

1880	M	Tg(swe+V717F)8 +/- (C3H/C57F1)	12	SBRC
1826	M	Tg(swe+V717F)8 +/- (C3H/C57F1)	12	SBRC
1820	F	Tg(swe+V717F)8 -/- (C3H/C57F1)	12	SBRC
1832	F	Tg(swe+V717F)8 -/- (C3H/C57F1)	12	SBRC
34174	M	Tg(swe+V717F)8 -/- (C3H/C57F1)	12	CRND
232	M	Tg(swe+V717F)8 -/- (C3H/C57F1)	12	SBRC
217	M	Tg(swe+V717F)8 -/- (C3H/C57F1)	12	SBRC
1861	M	Tg(swe+V717F)8 +/- (C3H/C57F1)	12	SBRC
214	M	Tg(swe+V717F)8 -/- (C3H/C57F1)	12	SBRC
273	F	Tg(swe+V717F)8 -/- (C3H/C57F1)	3	SBRC
274	F	Tg(swe+V717F)8 -/- (C3H/C57F1)	3	SBRC
275	F	Tg(swe+V717F)8 -/- (C3H/C57F1)	3	SBRC
276	F	Tg(swe+V717F)8 -/- (C3H/C57F1)	3	SBRC
277	F	Tg(swe+V717F)8 -/- (C3H/C57F1)	3	SBRC
278	F	Tg(swe+V717F)8 -/- (C3H/C57F1)	3	SBRC
283	F	Tg(swe+V717F)8 -/- (C3H/C57F1)	3	SBRC
284	F	Tg(swe+V717F)8 -/- (C3H/C57F1)	3	SBRC
280	M	Tg(swe+V717F)8 -/- (C3H/C57F1)	3	SBRC
287	M	Tg(swe+V717F)8 -/- (C3H/C57F1)	3	SBRC
30612	M	Tg(swe+V717F)8 -/- (C3H/C57F1)	3	SBRC
30614	M	Tg(swe+V717F)8 -/- (C3H/C57F1)	3	SBRC
30634	M	Tg(swe+V717F)8 -/- (C3H/C57F1)	3	SBRC
30635	M	Tg(swe+V717F)8 -/- (C3H/C57F1)	3	SBRC
30636	M	Tg(swe+V717F)8 -/- (C3H/C57F1)	3	SBRC
30637	M	Tg(swe+V717F)8 -/- (C3H/C57F1)	3	SBRC
281	F	Tg(swe+V717F)8 +/- (C3H/C57F1)	3	SBRC
282	F	Tg(swe+V717F)8 +/- (C3H/C57F1)	3	SBRC
285	F	Tg(swe+V717F)8 +/- (C3H/C57F1)	3	SBRC
30616	F	Tg(swe+V717F)8 +/- (C3H/C57F1)	3	SBRC
30617	F	Tg(swe+V717F)8 +/- (C3H/C57F1)	3	SBRC
31492	F	Tg(swe+V717F)8 +/- (C3H/C57F1)	3	SBRC
31495	F	Tg(swe+V717F)8 +/- (C3H/C57F1)	3	SBRC
30664	F	Tg(swe+V717F)8 +/- (C3H/C57F1)	3	SBRC
30665	F	Tg(swe+V717F)8 +/- (C3H/C57F1)	3	SBRC
286	M	Tg(swe+V717F)8 +/- (C3H/C57F1)	3	SBRC
31822	M	Tg(swe+V717F)8 +/- (C3H/C57F1)	3	SBRC
31823	M	Tg(swe+V717F)8 +/- (C3H/C57F1)	3	SBRC
31825	M	Tg(swe+V717F)8 +/- (C3H/C57F1)	3	SBRC

Legend: M=male, F=female, CRND=Center for Research in Neurodegenerative Diseases, SBRC= St. Boniface Research Center

LIST OF REFERENCES

Alzheimer's.Association (2008) "2008 Alzheimer's Disease Facts and Figures."

Alzheimer's.Association. (2009). from www.alz.org.

Alzheimer, A. (1906). "Über einen eigenartigen schweren

Erkrankungsprozeß der Hirnrinde. ." Neurologisches Centralblatt(23): 1129–36.

Alzheimer, A. (1907). "Über eine eigenartige Erkrankung der Hirnrinde." Allegmine Zeitschrift für Psychiatrie und Psychisch-Gerichtliche Medizin(64): 146–48.

Alzheimer.Society.of.Canada. (2011). from http://www.alzheimer.ca.

Amsel, A. (1993). "Hippocampal function in the rat: cognitive mapping or vicarious trial and error?" Hippocampus **3**(3): 251-6.

Andersen, O. M., J. Reiche, et al. (2005). "Neuronal sorting protein-related receptor sorLA/LR11 regulates processing of the amyloid precursor protein." Proc Natl Acad Sci U S A **102**(38): 13461-6.

Arai, T., K. Ikeda, et al. (2001). "Distinct isoforms of tau aggregated in neurons and glial cells in brains of patients with Pick's disease, corticobasal degeneration and progressive supranuclear palsy." Acta Neuropathol **101**(2): 167-73.

Arendash, G. W., D. L. King, et al. (2001). "Progressive, age-related behavioral impairments in transgenic mice carrying both mutant amyloid precursor protein and presenilin-1 transgenes." Brain Res **891**(1-2): 42-53.

Bertram, L. and R. E. Tanzi (2008). "Thirty years of Alzheimer's disease genetics: the implications of systematic meta-analyses." Nat Rev Neurosci **9**(10): 768-78.

Bilbul, M. and H. M. Schipper (2011). "Risk profiles of Alzheimer disease." Can J Neurol Sci **38**(4): 580-92.

Billings, L. M., S. Oddo, et al. (2005). "Intraneuronal Abeta causes the onset of early Alzheimer's disease-related cognitive deficits in transgenic mice." Neuron **45**(5): 675-88.

Bird, T. D. (2008). "Genetic aspects of Alzheimer disease." Genet Med **10**(4): 231-9.

Boada, M., C. Antunez, et al. (2010). "CALHM1 P86L polymorphism is associated with late-onset Alzheimer's disease in a recessive model." J Alzheimers Dis **20**(1): 247-51.

Braak, e. a. (1986). "Occurrence of neuropil threads in the senile human brain and in Alzheimer's disease: a third location of paired helical filaments outside of neurofibrillary tangles and neuritic plaques." Neuroscience letters **65**: 351.

Brody, D. L. and D. M. Holtzman (2006). "Morris water maze search strategy analysis in PDAPP mice before and after experimental traumatic brain injury." Exp Neurol **197**(2): 330-40.

Burns, A., E. J. Byrne, et al. (2002). "Alzheimer's disease." The Lancet **360**(9327): 163-165.

Campion, D., C. Dumanchin, et al. (1999). "Early-onset autosomal dominant Alzheimer disease: prevalence, genetic heterogeneity, and mutation spectrum." Am J Hum Genet **65**(3): 664-70.

Carlo Lovati, [5] Daniela Galimberti,[2,5] Diego Albani,[3,5] Pierluigi Bertora,[1] Eliana Venturelli,[2] Giuliana Cislaghi,[1] Ilaria Guidi,[2] Chiara Fenoglio,[2] Francesca Cortini,[2] Francesca Clerici,[1] Dario Finazzi,[4] Gianluigi Forloni,[3] Elio Scarpini,[2] and Claudio Mariani[1] (2010). "APOE ε2 and ε4 influence the susceptibility for Alzheimer's disease but not other dementias." International Journal of Molecular Epidemiololgy and Genetics
193 - 200.

Chartier-Harlin, M. C., F. Crawford, et al. (1991). "Early-onset Alzheimer's disease caused by mutations at codon 717 of the beta-amyloid precursor protein gene." Nature **353**(6347): 844-6.

Chishti, M. A., D. S. Yang, et al. (2001). "Early-onset amyloid deposition and cognitive deficits in transgenic mice expressing a double mutant form of amyloid precursor protein 695." J Biol Chem **276**(24): 21562-70.

Clarke, R., A. D. Smith, et al. (1998). "Folate, vitamin B12, and serum total homocysteine levels in confirmed Alzheimer disease." Arch Neurol **55**(11): 1449-55.

Cook, D. G., J. B. Leverenz, et al. (2003). "Reduced hippocampal insulin-degrading enzyme in late-onset Alzheimer's disease is associated with the apolipoprotein E-epsilon4 allele." Am J Pathol **162**(1): 313-9.

Crowe, M., R. Andel, et al. (2003). "Does participation in leisure activities lead to reduced risk of Alzheimer's disease? A prospective study of Swedish twins." J Gerontol B Psychol Sci Soc Sci **58**(5): P249-55.

Cummings, J. L. and G. Cole (2002). "Alzheimer disease." JAMA **287**(18): 2335-8.

D'Hooge, R., F. Franck, et al. (1999). "Age-related behavioural deficits in transgenic mice expressing the HIV-1 coat protein gp120." Eur J Neurosci **11**(12): 4398-402.

Delacourte, A., J. P. David, et al. (1999). "The biochemical pathway of neurofibrillary degeneration in aging and Alzheimer's disease." Neurology **52**(6): 1158-65.

Delacourte, A., N. Sergeant, et al. (1998). "Vulnerable neuronal subsets in Alzheimer's and Pick's disease are distinguished by their tau isoform distribution and phosphorylation." Ann Neurol **43**(2): 193-204.

Depboylu, C., F. Lohmuller, et al. (2006). "Alpha2-macroglobulin, lipoprotein receptor-related protein and lipoprotein receptor-associated protein and the genetic risk for developing Alzheimer's disease." Neurosci Lett **400**(3): 187-90.

Dickson, D. W. (1997). "The pathogenesis of senile plaques." J Neuropathol Exp Neurol **56**(4): 321-39.

Dineley, K. T., X. Xia, et al. (2002). "Accelerated plaque accumulation, associative learning deficits, and up-regulation of alpha 7 nicotinic receptor protein in transgenic mice co-expressing mutant human presenilin 1 and amyloid precursor proteins." J Biol Chem **277**(25): 22768-80.

Dodson, S. E., M. Gearing, et al. (2006). "LR11/SorLA expression is reduced in sporadic Alzheimer disease but not in familial Alzheimer disease." J Neuropathol Exp Neurol **65**(9): 866-72.

Doty, F. D., G. Entzminger, Jr., et al. (1999). "Practical aspects of birdcage coils." J Magn Reson **138**(1): 144-54.

Dreses-Werringloer, U., J. C. Lambert, et al. (2008). "A polymorphism in CALHM1 influences Ca2+ homeostasis, Abeta levels, and Alzheimer's disease risk." Cell **133**(7): 1149-61.

Duyckaerts, C., M.-C. Potier, et al. (2008). "Alzheimer disease models and human neuropathology: similarities and differences." Acta Neuropathologica **115**(1): 5-38.

Elder, G. A., M. A. Gama Sosa, et al. (2010). "Transgenic mouse models of Alzheimer's disease." Mt Sinai J Med **77**(1): 69-81.

Esch, F. S., P. S. Keim, et al. (1990). "Cleavage of amyloid beta peptide during constitutive processing of its precursor." Science **248**(4959): 1122-4.

Eskelinen, M. H., T. Ngandu, et al. (2009). "Midlife coffee and tea drinking and the risk of late-life dementia: a population-based CAIDE study." J Alzheimers Dis **16**(1): 85-91.

Farris, W., S. Mansourian, et al. (2003). "Insulin-degrading enzyme regulates the levels of insulin, amyloid beta-protein, and the beta-amyloid precursor protein intracellular domain in vivo." Proc Natl Acad Sci U S A **100**(7): 4162-7.

Ford, A. H., L. Flicker, et al. (2010). "Vitamins B(12), B(6), and folic acid for cognition in older men." Neurology **75**(17): 1540-7.

Gakhar-Koppole, N., P. Hundeshagen, et al. (2008). "Activity requires soluble amyloid precursor protein alpha to promote neurite outgrowth in neural stem cell-derived neurons via activation of the MAPK pathway." Eur J Neurosci **28**(5): 871-82.

Games, D., M. Buttini, et al. (2006). "Mice as models: transgenic approaches and Alzheimer's disease." J Alzheimers Dis **9**(3 Suppl): 133-49.

Gass, P., D. P. Wolfer, et al. (1998). "Deficits in memory tasks of mice with CREB mutations depend on gene dosage." Learn Mem **5**(4-5): 274-88.

Glazner, K. A., G. L. Odero, et al. (2010). "Strain specific differences in memory and neuropathology in a mouse model of Alzheimer's disease." Life Sci **86**(25-26): 942-50.

Gotz, J., F. Chen, et al. (2001). "Formation of neurofibrillary tangles in P301l tau transgenic mice induced by Abeta 42 fibrils." Science **293**(5534): 1491-5.

Graeber, M. B. (2003). "Alois Alzheimer (1864-1915)." Retrieved January 3, 2009, from http://www.ibro.info/media/pdf/si-his-pdf-pdf9.pdf.

Graziano, A., L. Petrosini, et al. (2003). "Automatic recognition of explorative strategies in the Morris water maze." J Neurosci Methods **130**(1): 33-44.

Grundke-Iqbal, I., K. Iqbal, et al. (1986). "Microtubule-associated protein tau. A component of Alzheimer paired helical filaments." J. Biol. Chem. **261**(13): 6084-6089.

Hardy, J. and D. J. Selkoe (2002). "The amyloid hypothesis of Alzheimer's disease: progress and problems on the road to therapeutics." Science **297**(5580): 353-6.

Hartmann, T., S. C. Bieger, et al. (1997). "Distinct sites of intracellular production for Alzheimer's disease A beta40/42 amyloid peptides." Nat Med **3**(9): 1016-20.

Holcomb, L., M. N. Gordon, et al. (1998). "Accelerated Alzheimer-type phenotype in transgenic mice carrying both mutant amyloid precursor protein and presenilin 1 transgenes." Nat Med **4**(1): 97-100.

Hollenbach, E., S. Ackermann, et al. (1998). "Confirmation of an association between a polymorphism in exon 3 of the low-density lipoprotein receptor-related protein gene and Alzheimer's disease." Neurology **50**(6): 1905-7.

Hsiao, K., P. Chapman, et al. (1996). "Correlative memory deficits, Abeta elevation, and amyloid plaques in transgenic mice." Science **274**(5284): 99-102.

Illenberger, S., Q. Zheng-Fischhofer, et al. (1998). "The endogenous and cell cycle-dependent phosphorylation of tau protein in living cells: implications for Alzheimer's disease." Mol Biol Cell **9**(6): 1495-512.

Iwata, N., S. Tsubuki, et al. (2000). "Identification of the major Abeta1-42-degrading catabolic pathway in brain parenchyma: suppression leads to biochemical and pathological deposition." Nat Med **6**(2): 143-50.

Janus, C. (2004). "Search strategies used by APP transgenic mice during navigation in the Morris water maze." Learn Mem **11**(3): 337-46.

Johnston, J. A., R. F. Cowburn, et al. (1994). "Increased beta-amyloid release and levels of amyloid precursor protein (APP) in fibroblast cell lines from family members with the Swedish Alzheimer's disease APP670/671 mutation." FEBS Lett **354**(3): 274-8.

Kaether, C., C. Haass, et al. (2006). "Assembly, trafficking and function of gamma-secretase." Neurodegener Dis **3**(4-5): 275-83.

Kalaria, R. N. (2000). "The role of cerebral ischemia in Alzheimer's disease." Neurobiol Aging **21**(2): 321-30.

Kang, D. E., T. Saitoh, et al. (1997). "Genetic association of the low-density lipoprotein receptor-related protein gene (LRP), an apolipoprotein E receptor, with late-onset Alzheimer's disease." Neurology **49**(1): 56-61.

Kang, J., H. G. Lemaire, et al. (1987). "The precursor of Alzheimer's disease amyloid A4 protein resembles a cell-surface receptor." Nature **325**(6106): 733-6.

Kantarci, K., C. R. Jack, Jr., et al. (2001). "Mild cognitive impairment and Alzheimer disease: regional diffusivity of water." Radiology **219**(1): 101-7.

Kantarci, K., R. C. Petersen, et al. (2005). "DWI predicts future progression to Alzheimer disease in amnestic mild cognitive impairment." Neurology **64**(5): 902-4.

Khachaturian, A. S., C. D. Corcoran, et al. (2004). "Apolipoprotein E epsilon4 count affects age at onset of Alzheimer disease, but not lifetime susceptibility: The Cache County Study." Arch Gen Psychiatry **61**(5): 518-24.

Kivipelto, M., E. L. Helkala, et al. (2002). "Apolipoprotein E epsilon4 allele, elevated midlife total cholesterol level, and high midlife systolic blood pressure are independent risk factors for late-life Alzheimer disease." Ann Intern Med **137**(3): 149-55.

Kivipelto, M., E. L. Helkala, et al. (2001). "Midlife vascular risk factors and Alzheimer's disease in later life: longitudinal, population based study." BMJ **322**(7300): 1447-51.

Kovacs, D. M. (2000). "alpha2-macroglobulin in late-onset Alzheimer's disease." Exp Gerontol **35**(4): 473-9.

Lambert, J. C. and P. Amouyel (2011). "Genetics of Alzheimer's disease: new evidences for an old hypothesis?" Curr Opin Genet Dev **21**(3): 295-301.

Larner, A. J. and M. Doran (2006). "Clinical phenotypic heterogeneity of Alzheimer's disease associated with mutations of the presenilin-1 gene." J Neurol **253**(2): 139-58.

Larrieu, S., L. Letenneur, et al. (2004). "Nutritional factors and risk of incident dementia in the PAQUID longitudinal cohort." J Nutr Health Aging **8**(3): 150-4.

Lee, V. M.-Y. (2001). "BIOMEDICINE: Enhanced: Tauists and baptists United--Well Almost!" Science **293**(5534): 1446-1447.

Levy-Lahad, E., W. Wasco, et al. (1995). "Candidate gene for the chromosome 1 familial Alzheimer's disease locus." Science **269**(5226): 973-7.

Lewis, J., D. W. Dickson, et al. (2001). "Enhanced neurofibrillary degeneration in transgenic mice expressing mutant tau and APP." Science **293**(5534): 1487-91.

Lewis, J., E. McGowan, et al. (2000). "Neurofibrillary tangles, amyotrophy and progressive motor disturbance in mice expressing mutant (P301L) tau protein." Nat Genet **25**(4): 402-5.

Lichtenthaler, S. F. (2011). "Alpha-Secretase Cleavage of the Amyloid Precursor Protein: Proteolysis Regulated by Signaling Pathways and Protein Trafficking." Curr Alzheimer Res.

Lovati, C., D. Galimberti, et al. (2010). "APOE ε2 and ε4 influence the susceptibility for Alzheimer's disease but not other dementias." International Journal of Molecular Epidemiololgy and Genetics

193 - 200.

Maccioni, R. B., J. P. Muñoz, et al. (2001). "The Molecular Bases of Alzheimer's Disease and Other Neurodegenerative Disorders." Archives of Medical Research **32**(5): 367-381.

MacKenzie-Graham, A., E. F. Lee, et al. (2004). "A multimodal, multidimensional atlas of the C57BL/6J mouse brain." J Anat **204**(2): 93-102.

Maia, L. and A. de Mendonca (2002). "Does caffeine intake protect from Alzheimer's disease?" Eur J Neurol **9**(4): 377-82.

Markesbery, W. R. (1997). "Neuropathological criteria for the diagnosis of Alzheimer's disease." Neurobiol Aging **18**(4 Suppl): S13-9.

Marx, J. (2007). "ALZHEIMER'S DISEASE: A New Take on Tau." Science **316**(5830): 1416-1417.

Mattson, M. P. (1997). "Cellular actions of beta-amyloid precursor protein and its soluble and fibrillogenic derivatives." Physiol Rev **77**(4): 1081-132.

McDermott, J. R. and A. M. Gibson (1997). "Degradation of Alzheimer's beta-amyloid protein by human and rat brain peptidases: involvement of insulin-degrading enzyme." Neurochem Res **22**(1): 49-56.

Means, L. W., J. L. Higgins, et al. (1993). "Mid-life onset of dietary restriction extends life and prolongs cognitive functioning." Physiol Behav **54**(3): 503-8.

Miller, B. C., E. A. Eckman, et al. (2003). "Amyloid-beta peptide levels in brain are inversely correlated with insulysin activity levels in vivo." Proc Natl Acad Sci U S A **100**(10): 6221-6.

Morris, R. (1984). "Developments of a water-maze procedure for studying spatial learning in the rat." J Neurosci Methods **11**(1): 47-60.

Narita, M., D. M. Holtzman, et al. (1997). "Alpha2-macroglobulin complexes with and mediates the endocytosis of beta-amyloid peptide via cell surface low-density lipoprotein receptor-related protein." J Neurochem **69**(5): 1904-11.

Oddo, S., A. Caccamo, et al. (2003a). "Amyloid deposition precedes tangle formation in a triple transgenic model of Alzheimer's disease." Neurobiol Aging **24**(8): 1063-70.

Oddo, S., A. Caccamo, et al. (2003b). "Triple-transgenic model of Alzheimer's disease with plaques and tangles: intracellular Abeta and synaptic dysfunction." Neuron **39**(3): 409-21.

Offe, K., S. E. Dodson, et al. (2006). "The lipoprotein receptor LR11 regulates amyloid beta production and amyloid precursor protein traffic in endosomal compartments." J Neurosci **26**(5): 1596-603.

Patil, S. S., F. Schlick, et al. (2009). "Involvement of individual hippocampal signaling protein levels in spatial memory formation is strain-dependent." Amino Acids.

Peila, R., B. L. Rodriguez, et al. (2002). "Type 2 diabetes, APOE gene, and the risk for dementia and related pathologies: The Honolulu-Asia Aging Study." Diabetes **51**(4): 1256-62.

Perez, A., L. Morelli, et al. (2000). "Degradation of soluble amyloid beta-peptides 1-40, 1-42, and the Dutch variant 1-40Q by insulin degrading enzyme from Alzheimer disease and control brains." Neurochem Res **25**(2): 247-55.

Qiu, W. Q., W. Borth, et al. (1996). "Degradation of amyloid beta-protein by a serine protease-alpha2-macroglobulin complex." J Biol Chem **271**(14): 8443-51.

Reilly, J. F., D. Games, et al. (2003). "Amyloid deposition in the hippocampus and entorhinal cortex: quantitative analysis of a transgenic mouse model." Proc Natl Acad Sci U S A **100**(8): 4837-42.

Roberts, G. W. (1988). "Immunocytochemistry of neurofibrillary tangles in dementia pugilistica and Alzheimer's disease: evidence for common genesis." Lancet **2**(8626-8627): 1456-8.

Rogaev, E. I., R. Sherrington, et al. (1995). "Familial Alzheimer's disease in kindreds with missense mutations in a gene on chromosome 1 related to the Alzheimer's disease type 3 gene." Nature **376**(6543): 775-8.

Rogaeva, E., Y. Meng, et al. (2007). "The neuronal sortilin-related receptor SORL1 is genetically associated with Alzheimer disease." Nat Genet **39**(2): 168-77.

Rovio, S., I. Kareholt, et al. (2005). "Leisure-time physical activity at midlife and the risk of dementia and Alzheimer's disease." Lancet Neurol **4**(11): 705-11.

Scherzer, C. R., K. Offe, et al. (2004). "Loss of apolipoprotein E receptor LR11 in Alzheimer disease." Arch Neurol **61**(8): 1200-5.

Scheuner, D., C. Eckman, et al. (1996). "Secreted amyloid beta-protein similar to that in the senile plaques of Alzheimer's disease is increased in vivo by the presenilin 1 and 2 and APP mutations linked to familial Alzheimer's disease." Nat Med **2**(8): 864-70.

Sebastiani, G., P. Krzywkowski, et al. (2006). "Mapping genetic modulators of amyloid plaque deposition in TgCRND8 transgenic mice." Hum Mol Genet **15**(15): 2313-23.

Selkoe, D. J. (2001). "Alzheimer's Disease: Genes, Proteins, and Therapy." Physiol. Rev. **81**(2): 741-766.
Selkoe, D. J. (2001). "Presenilin, Notch, and the genesis and treatment of Alzheimer's disease." Proc Natl Acad Sci U S A **98**(20): 11039-41.
Selkoe, D. J. and M. B. Podlisny (2002). "Deciphering the genetic basis of Alzheimer's disease." Annu Rev Genomics Hum Genet **3**: 67-99.
Sherrington, R., E. I. Rogaev, et al. (1995). "Cloning of a gene bearing missense mutations in early-onset familial Alzheimer's disease." Nature **375**(6534): 754-60.
Sisodia, S. S. (1992). "Beta-amyloid precursor protein cleavage by a membrane-bound protease." Proc Natl Acad Sci U S A **89**(13): 6075-9.
Stejskal, E. O. and J. E. Tanner (1965). "Spin Diffusion Measurements: Spin Echoes in the Presence of a Time-Dependent Field Gradient." The Journal of Chemical Physics **42**(1): 288-292.
Sun, X., G. He, et al. (2006). "Hypoxia facilitates Alzheimer's disease pathogenesis by up-regulating BACE1 gene expression." Proc Natl Acad Sci U S A **103**(49): 18727-32.
Terry, R. D., N. K. Gonatas, et al. (1964). "The ultrastructure of the cerebral cortex in Alzheimer's disease." Trans Am Neurol Assoc **89**: 12.
Terry, R. D., L. A. Hansen, et al. (1987). "Senile dementia of the Alzheimer type without neocortical neurofibrillary tangles." J Neuropathol Exp Neurol **46**(3): 262-8.
Thiessen, J. D., K. A. Glazner, et al. (2010). "Histochemical visualization and diffusion MRI at 7 Tesla in the TgCRND8 transgenic model of Alzheimer's disease." Brain Struct Funct **215**(1): 29-36.
Thomas, D. L., G. S. Pell, et al. (1998). "A quantitative method for fast diffusion imaging using magnetization-prepared TurboFLASH." Magn Reson Med **39**(6): 950-60.
Tolman, E. C. (1948). "Cognitive maps in rats and men." Psychol Rev **55**: 1-4.
Tucker, K. L., B. Olson, et al. (2004). "Breakfast cereal fortified with folic acid, vitamin B-6, and vitamin B-12 increases vitamin concentrations and reduces homocysteine concentrations: a randomized trial." Am J Clin Nutr **79**(5): 805-11.
Tucker, R. P. (1990). "The roles of microtubule-associated proteins in brain morphogenesis: a review." Brain Res Brain Res Rev **15**(2): 101-20.
Tzourio, C., C. Anderson, et al. (2003). "Effects of blood pressure lowering with perindopril and indapamide therapy on dementia and cognitive decline in patients with cerebrovascular disease." Arch Intern Med **163**(9): 1069-75.
Valenzuela, M. J. and P. Sachdev (2006). "Brain reserve and dementia: a systematic review." Psychol Med **36**(4): 441-54.
Van Broeckhoven, C. L. (1995). "Molecular genetics of Alzheimer disease: identification of genes and gene mutations." Eur Neurol **35**(1): 8-19.
Wahlsten, D. (1982). "Deficiency of corpus callosum varies with strain and supplier of the mice." Brain Res **239**(2): 329-47.
Wall, S. L., HT(ASCP). (1996). Surgical Pathology - Histology Staining Manual - ThioFlavine S - Amyloid.
Wang, H. X., A. Wahlin, et al. (2001). "Vitamin B(12) and folate in relation to the development of Alzheimer's disease." Neurology **56**(9): 1188-94.

Wang, S., R. Wang, et al. (2010). "Expression and functional profiling of neprilysin, insulin-degrading enzyme, and endothelin-converting enzyme in prospectively studied elderly and Alzheimer's brain." J Neurochem **115**(1): 47-57.

Wehner, J. M., S. Sleight, et al. (1990). "Hippocampal protein kinase C activity is reduced in poor spatial learners." Brain Res **523**(2): 181-7.

Whitmer, R. A., S. Sidney, et al. (2005). "Midlife cardiovascular risk factors and risk of dementia in late life." Neurology **64**(2): 277-81.

Williams, D. R. and A. J. Lees (2009). "Progressive supranuclear palsy: clinicopathological concepts and diagnostic challenges." Lancet Neurol **8**(3): 270-9.

Wilson, R. S., K. R. Krueger, et al. (2007). "Loneliness and risk of Alzheimer disease." Arch Gen Psychiatry **64**(2): 234-40.

Wolfe, M. S. and S. Y. Guenette (2007). "APP at a glance." J Cell Sci **120**(Pt 18): 3157-61.

Wolfer, D. P. and H. P. Lipp (2000). "Dissecting the behaviour of transgenic mice: is it the mutation, the genetic background, or the environment?" Exp Physiol **85**(6): 627-34.